Calculation No: NSTXU-CALC-011-10-00 **Revision No: 0**

PFCs Analysis of the IBDH Tiles

Purpose of Calculation: (Define why the calculation is being performed.)

Verify that CSFW tiles Row 7 – Row 21 meet the structural design requirements when exposed to structural, thermal and electromagnetic loads.

Codes and versions: (List all codes, if any, used)

ANSYS v19.1

References (List any source of design information including computer program titles and revision levels.)

1) GENERAL REQUIREMENTS DOCUMENT NSTX-U-RQMT-GRD-001-02
2) NSTX-U SYSTEM REQUIREMENTS DOCUMENT Plasma Facing Components NSTX-U-RQMT-SRD-003-01 July 14, 2018
3) NSTX-U Disruption Analysis Requirements NSTX-U-RQMT-RD-003-02 7/23/18
4) NSTXU Recovery Global Heat Balance Calculations, NSTXU-CALC-10-06-00, by H Zhang

Assumptions (Identify all assumptions made as part of this calculation.)

1) The value of peak background fields and peak dBdts were taken from NSTXU-CALC-11-08-00. All assumptions described in the fields and dBdts document are valid for this analysis.

2) As described in the disruptions requirements document NSTX-U-RQMT-RD-003-00_Disruptions, halo currents are assumed to strike in a toroidal band of 20 cm poloidal width. The halo current incident on each tile was factored based on poloidal width of the tile.

3) Current is assumed to flow thru the conducting support structure into the casing. The casing face was grounded (zero volts) to represent this current flow.

Calculation (Calculation is either documented here or attached)

See attached report sections "Method of Analysis" and "Results"

Conclusion (Specify whether or not the purpose of the calculation was accomplished.)

The design meets fit, form and function requirements. See Section 6 for details.

Cognizant Individual (or designee) printed name, signature, and date

Ankita Jariwala

Preparer's printed name, signature and date

Wassee Syed Wassee Syed Digitally signed by Wassee Syed Date: 2018.09.27 11:33:20 -04'00'

I have reviewed this calculation and, to my professional satisfaction, it is properly performed and correct. Checker's

printed name, signature, and date

Arthur Brooks Art Brooks Digitally signed by Art Brooks Date: 2018.09.27 13:08:49 -04'00'

National Spherical Torus eXperiment - Upgrade

NSTX-U

Combined Load Calculation for CSFW Row 7 – Row 21

NSTXU-CALC-11-10-00

Sep 24, 2018

Wassee Syed
Digitally signed by Wassee Syed
Date: 2018.09.27 11:33:46 -04'00'

Prepared By
Wassee Syed / Nathan Dean

Art Brooks
Digitally signed by Art Brooks
Date: 2018.09.27 13:04:22 -04'00'

Reviewed By
Art Brooks

Michael Jaworski
Digitally signed by Michael Jaworski
Date: 2018.09.27 13:51:08 -04'00'

Approved By – Responsible Engineer
Michael Jaworski

Checks for Calculation No: NSTXU-CALC-11-10-00 **Revision No: 0**

Combined Load Calculation for CSFW Row 7 – Row 21

Component was checked against latest design

Yes

All required load cases are included and current

Yes

Discuss method used in the calculation

The use of ANSYS Workbench is considered an acceptable approach to analyzing problems of this type.

Discuss how the calculation was checked (*)

The calculation was checked by

1) comparing the inputs to the models as stated herein with the project requirements
2) comparing results with previous similar analyses of the CSFW
3) doing simpler local calculations on the effectiveness of adding grafoil bushings to reduce stress concentrations.

List issue identified and how they were resolved

High stress areas at the rod-tile interfaces found in initial analysis were mitigated by using Grafoil bushings, compliant material, to distribute loads and reduce local stresses.

Checker's name: Art Books

Technical Authority: Robert Ellis Digitally signed by Robert Ellis Date: 2018.09.27 14:42:34 -04'00' ______(sign and date)

(*) independent calculations can be appended

1. Minimum Requirements for Checking Calculations

2. Assure that inputs were correctly selected and incorporated into the design.

3. Calculation considers, as appropriate:

- Performance Requirements (capacity, rating, system output)
- Design Conditions (pressure, temperature, voltage, etc.)
- Load Conditions (Electromagnetic (Lorentz Force), seismic, wind, thermal, dynamic)
- Environmental Conditions (radiation zone, hazardous material, etc.)
- Material Requirements
- Structural Requirements (foundations, pipe supports, etc.)
- Hydraulic Requirements (NPSH, pressure drops, etc.)
- Chemistry Requirements
- Electrical Requirements (power source, volts, raceway, and insulation)
- Equipment Reliability (FMEA)
- Failure Effects on Surrounding Equipment
- Tolerance Buildup

4. Assumptions necessary to perform the design activity are adequately described and reasonable.

5. An appropriate calculation method was used.

6. The results are reasonable compared to the inputs.

7. Error bars (range) for inputs used, results / conclusions, assumptions, have been considered and are acceptable.

NOTE: IT IS THE RESPONSIBILITY OF THE CHECKER TO USE METHODS THAT WILL SUBSTANTIATE TO HIS/HER PROFESSIONAL SATISFACTION THAT THE CALCULATION IS CORRECT.

BY SIGNING CALCULATION, CHECKER ACKNOWLEDGES THAT THE CALCULATION HAS BEEN APPROPRIATELY CHECKED AND THAT THE APPLICABLE ITEMS LISTED ABOVE HAVE BEEN INCLUDED AS PART OF THE CHECK.

NSTX-U CALCULATION

Record of Changes

Rev.	Date	Description of Changes	Revised by
0	9/24/18	Initial Release	

Table of Contents

List of Figures

1 Executive Summary

This report documents the methodology and results of structural, thermal and electromagnetic Finite Element Analysis performed on PFCs (Plasma Facing Components) – CSFW Tiles rows 7 - 14. Electromagnetic loads were imported to a Multiphysics model, which also incorporated the effects from bolt preload and thermal ratcheting.

A detailed analysis was performed on the base tile geometry. Three additional geometries were selected and analyzed for conformance with form, fit and function.

2 Introduction

PFCs experience Lorentz forces induced by plasma disruptions. Fluctuations in electric and magnetic fields due to plasma disruptions induce eddy currents in the PFCs and the conductive support structures. Additionally, plasma contact with the PFCs may also generate halo currents. The halo currents strike the structure at one poloidal and toroidal location, flow thru the conductive structures and exit at another location.

The magnitudes and directions of the induced Lorentz loads depend on a number of factors including plasma shapes, movement, current decay, structure material properties, and geometry. Several assumptions must be made in order to determine "worst case" values for the Lorentz loads.

The halo currents also generate heat. After multiple halo current pulses, the temperature of the tiles can rise significantly above room temperature, resulting in stresses due to constrained thermal expansion.

The combined effect of thermal, electromagnetic and structural (bolt preload) loads must be studied to ensure that the stresses experienced by the tile assembly are within established allowable limits.

3 Method of Analysis

Separate Thermal and Electromagnetic analyses were conducted using ANSYS Mechanical and APDL respectively. The results from these analyses were imported to a structural model, which also included preload. The results from the structural model were used to determine the combined effect of the different types of loads.

3.1 Geometry and Materials

Figure 1 shows the labelled geometry and material specifications. The geometric symmetry of the tiles was taken advantage of, and a 30 degrees toroidal section was modelled. The material properties were taken from standard PPPL material database.

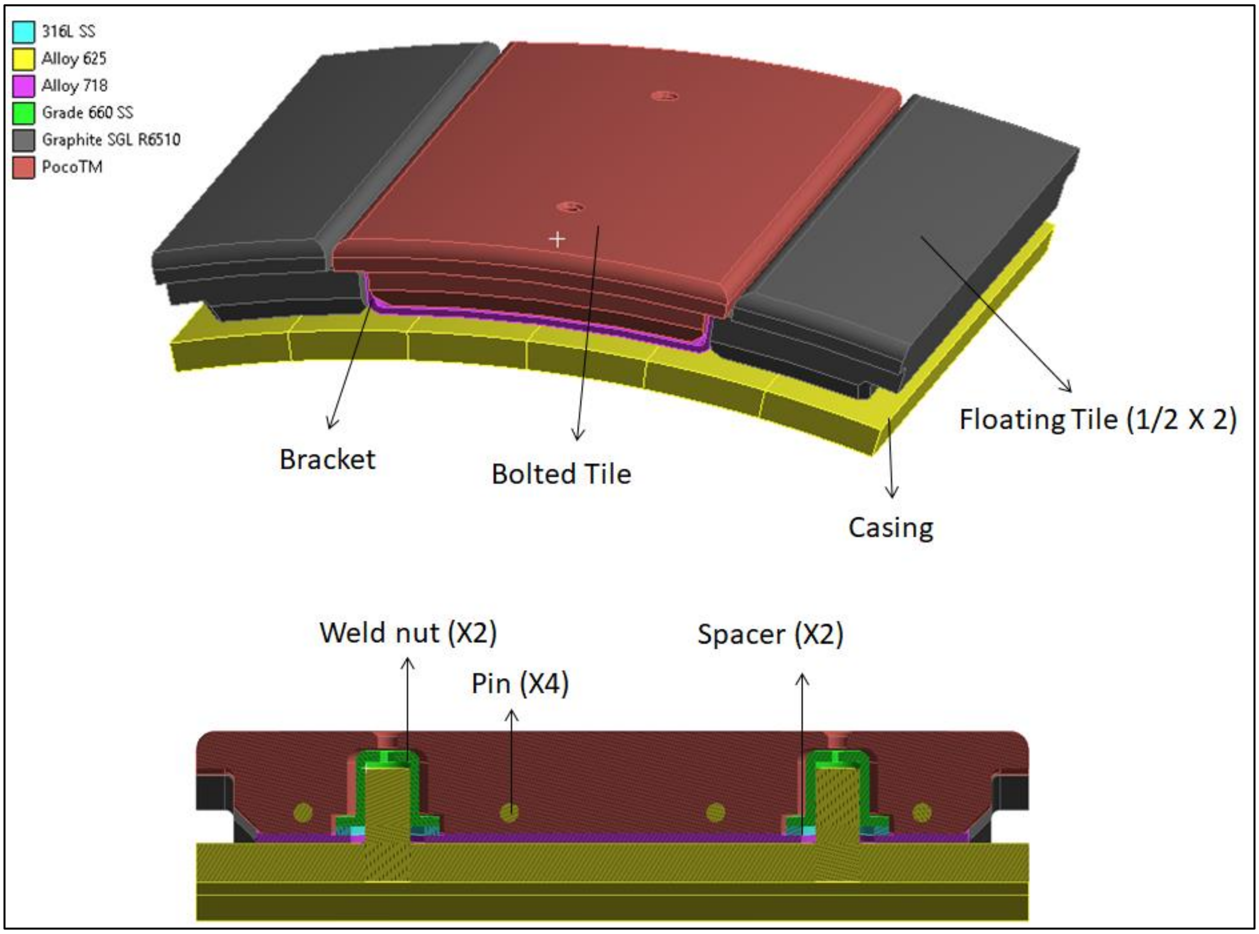

Figure 1: Geometry and Maetrials Specifications

3.2 Transient Thermal Analysis

3.2.1 FE Mesh

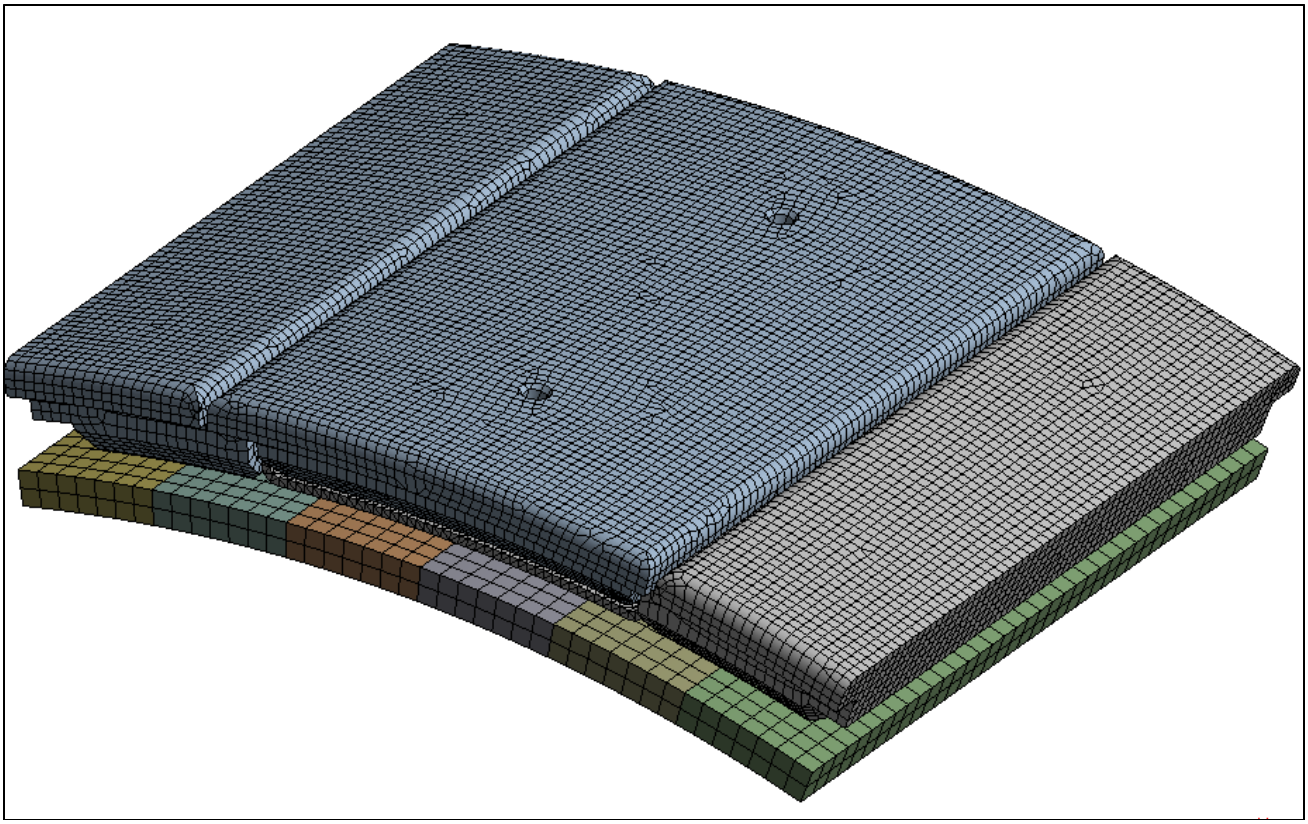

Figure 2: FE Mesh Thermal Model

3.2.2 <u>Contact Definitions</u>

Bonded contact was defined at threaded interfaces as shown in Figure 3.

Frictional contacts with a coefficient of friction of 0.15 were defined at the following interfaces (Metal – Metal):

- Washer - Weld Nut
- Washer - Bracket
- Bracket - Casing

These interfaces are highlighted in Figure 4.

Frictional contact with a coefficient of friction of 0.10 was defined between the pins and pin slots (Metal – Graphite). All other interfaces were defined as frictionless.

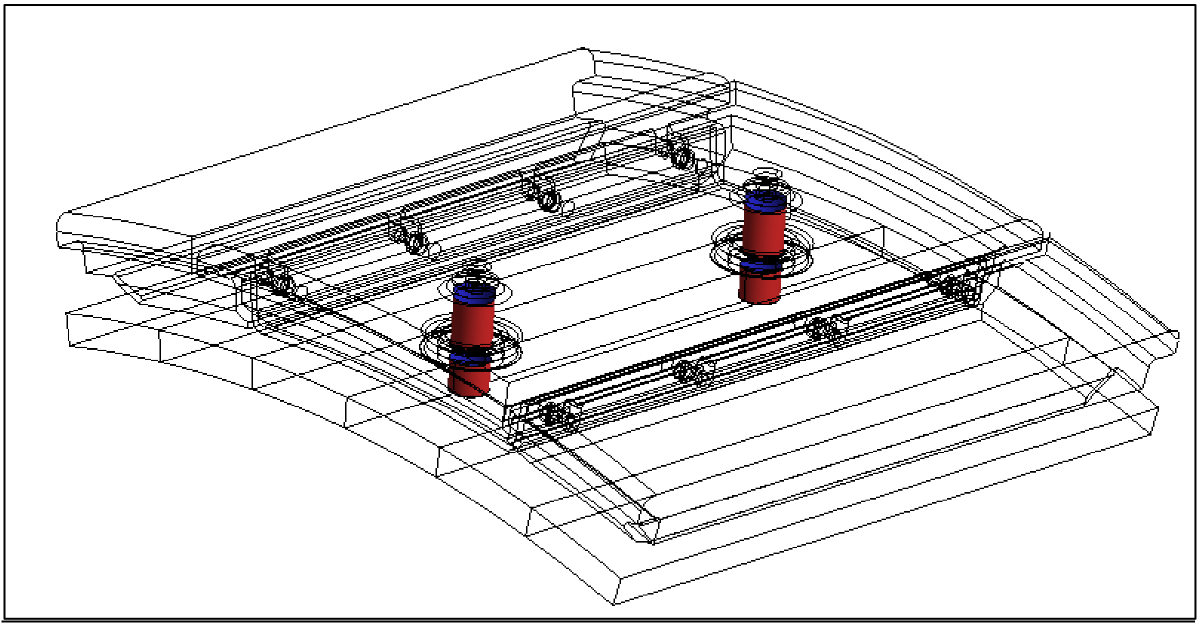

Figure 3: Bonded Contacts

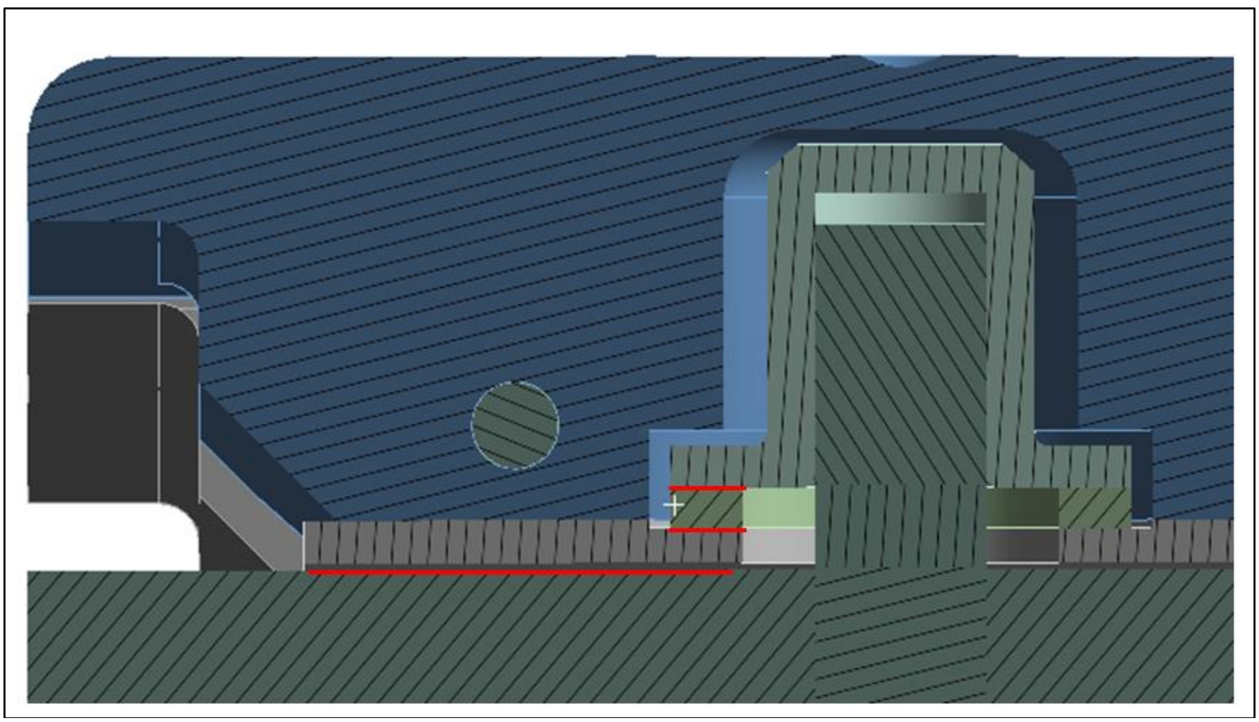

Figure 4: Frictional Contact with 0.15 COF

3.2.3 Boundary Conditions and Loads

Heat flux from halo loads acts on the tile top surfaces. The emissivity for radiation heat transfer was assumed to be 0.70, with an ambient temperature of 112.7 C (See referenced thermal analysis memo for determination of 112.7 C).

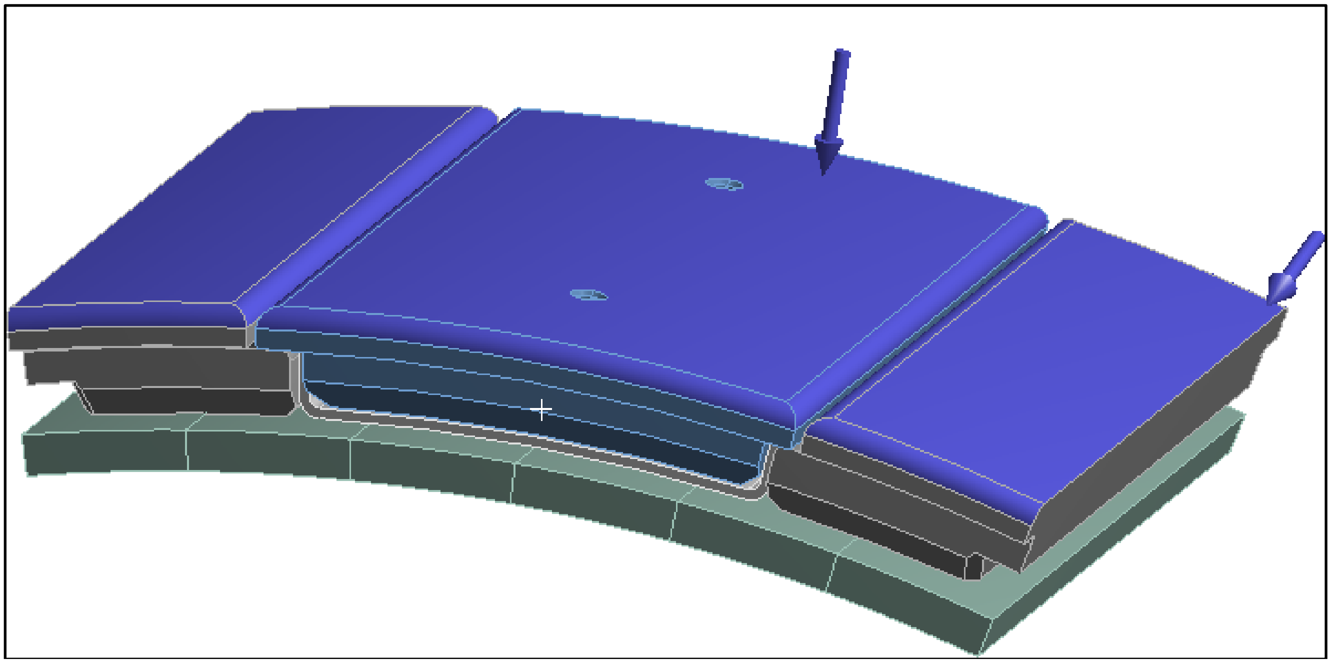

Figure 5: Heat flux Surfaces

The heat flux was applied in multiple 5 second pulses, with a 20 minute cool down period between the pulses. The number of pulses was determined by the ability of the system to shakedown to a constant maximum temperature. This will be discussed further under the results section.

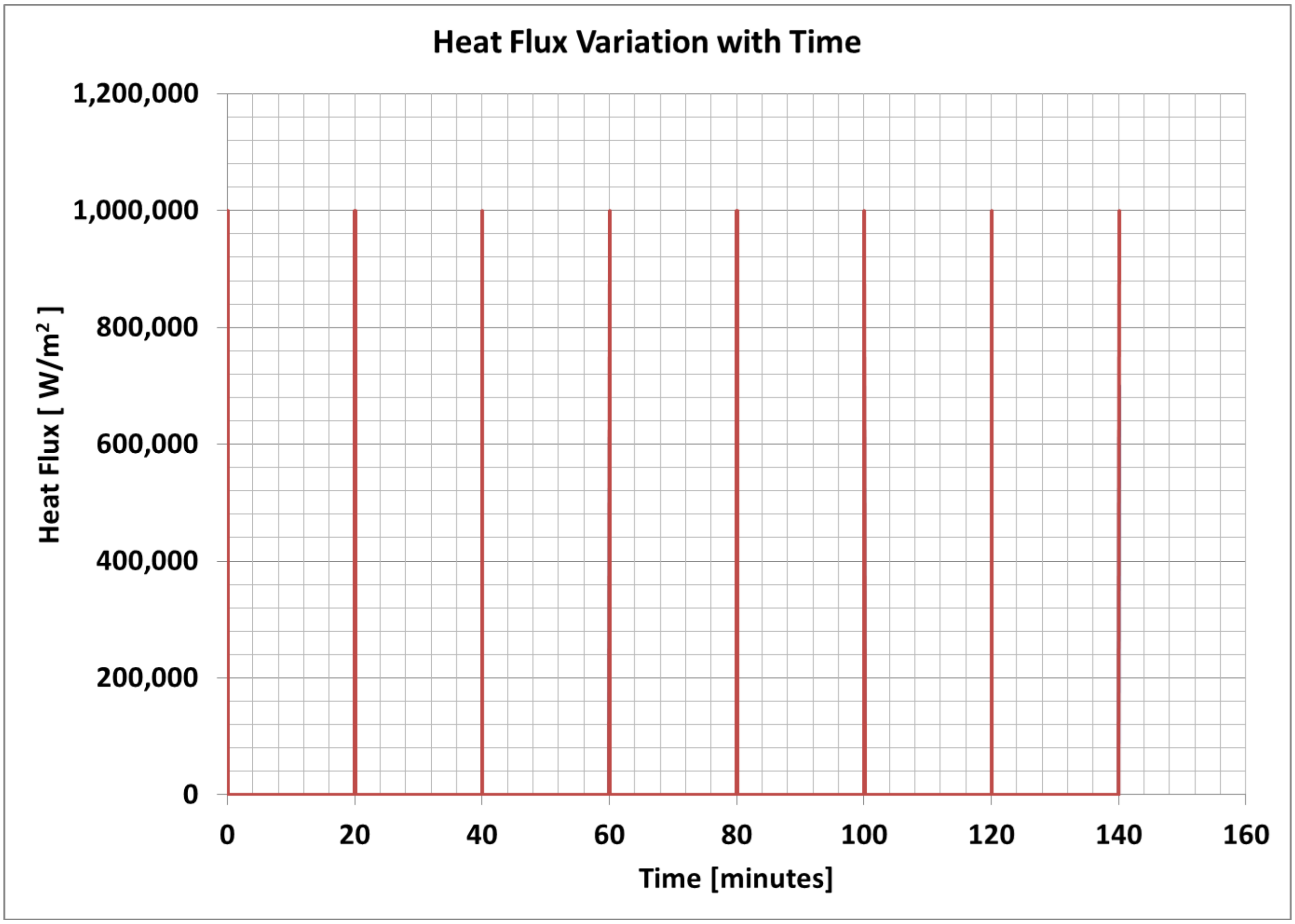

Figure 6: Heat Flux Application

3.2.4 Results

Figure 7 shows the temperature history for the PFC assembly. It can be seen that the maximum temperature stabilizes at 588 C, after the fourth pulse. The minimum temperature reaches 200 C. Temperature distribution plots are shown in Figure 8 and Figure 9.

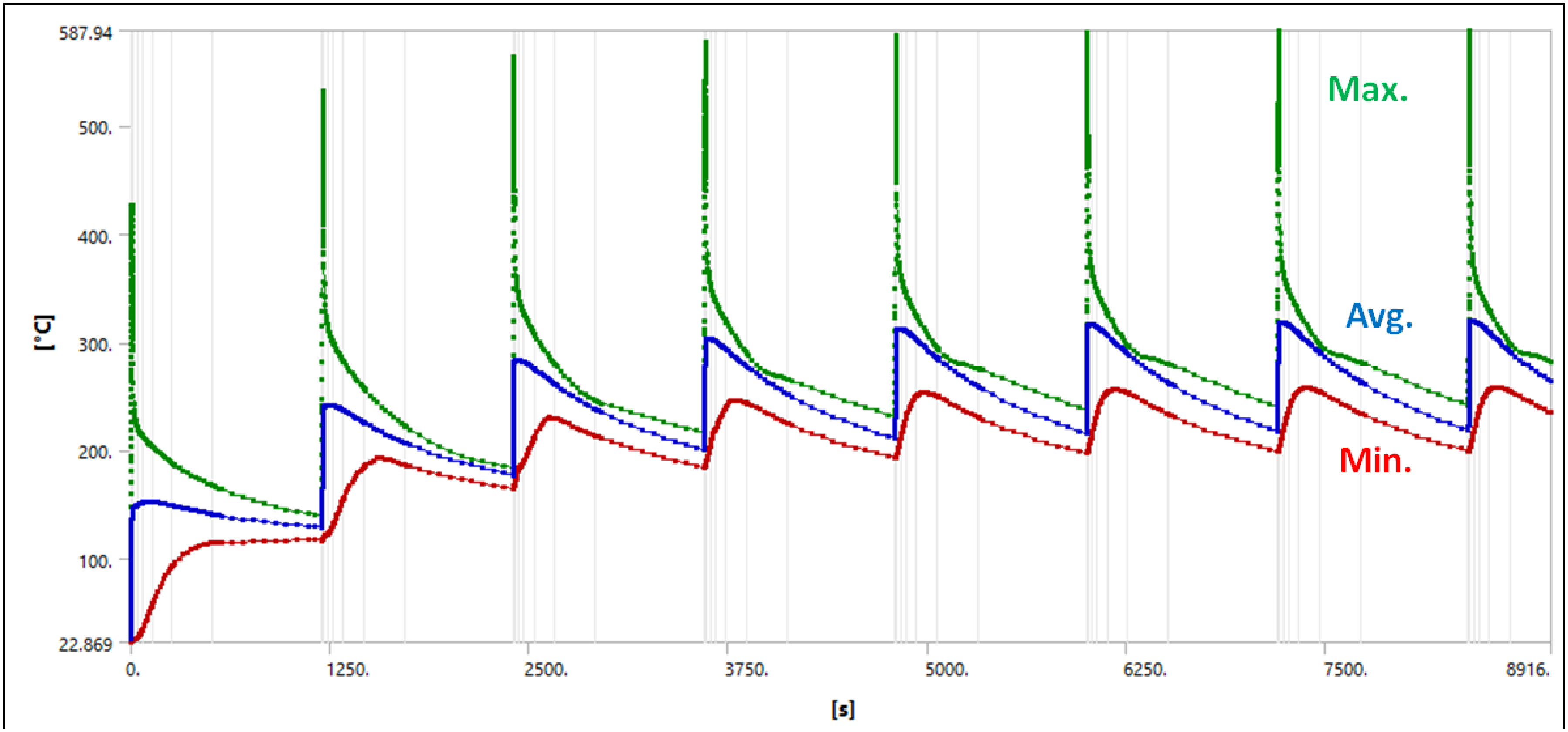

Figure 7: Temperature History, Tile Assembly

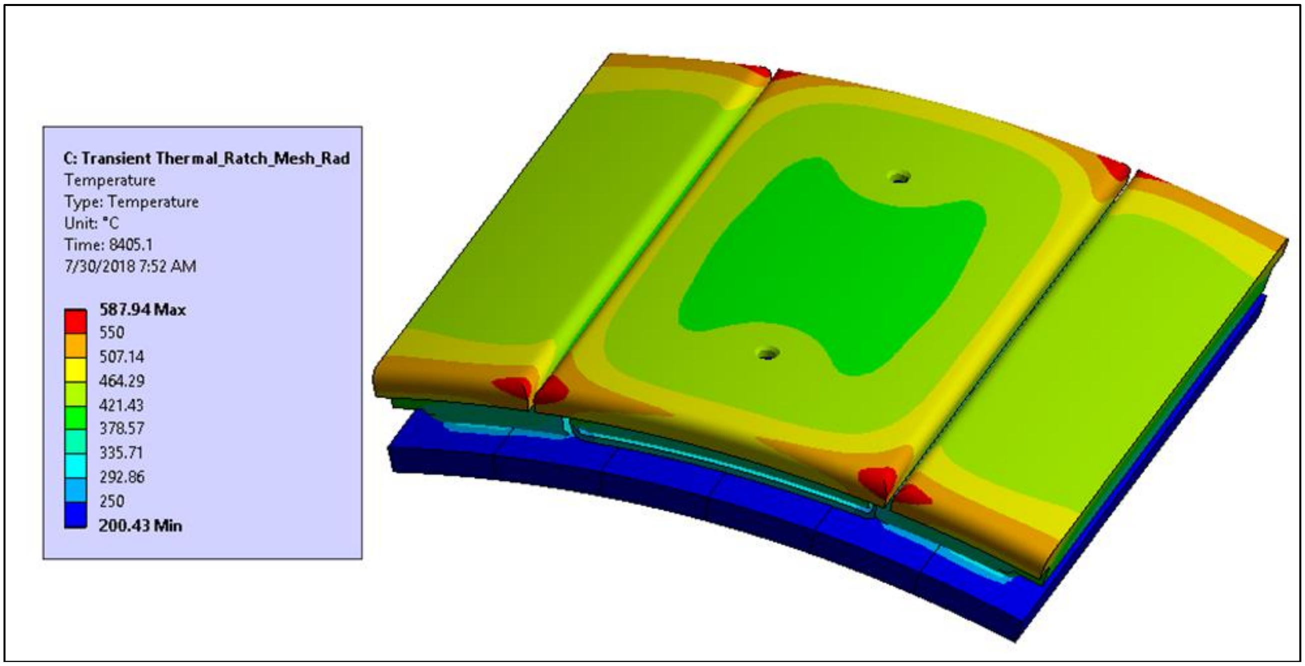

Figure 8: Temperature Distribution, Last Pulse Peak

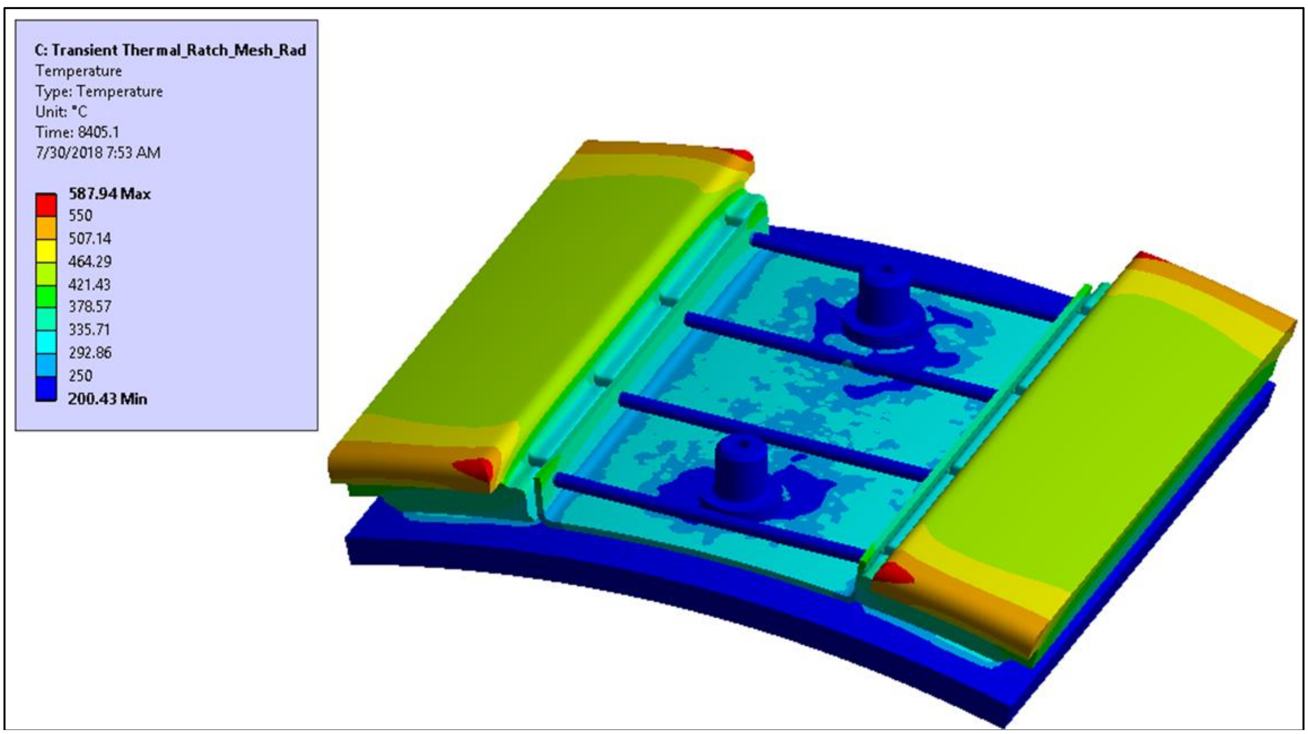

Figure 9: Temperature Distribution, Last Pulse Peak- Bolted Tile Hidden

3.3 Electromagnetic Analysis

3.3.1 FE Mesh

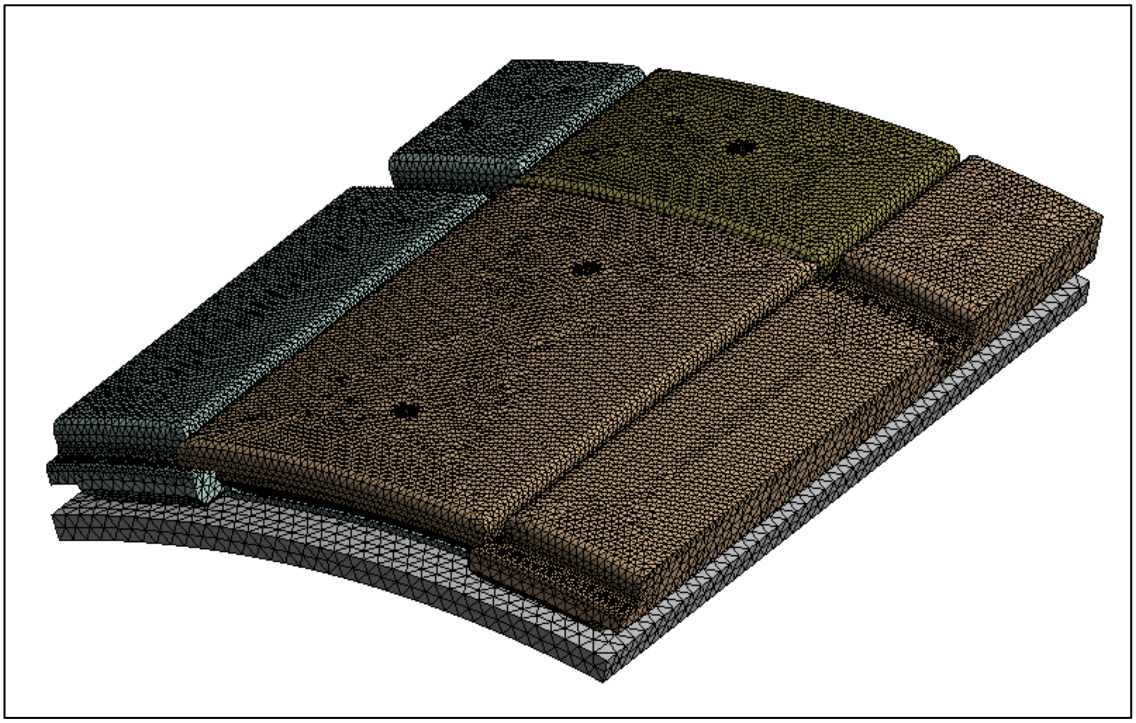

Figure 10: CSFW Mesh

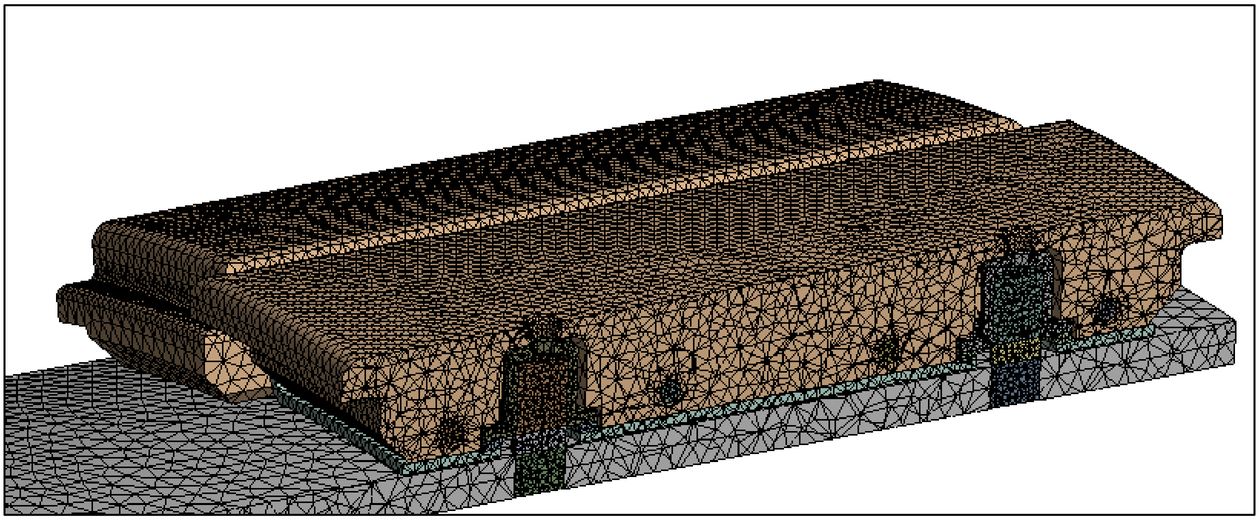

Figure 11: CSFW Mesh Cross Section

SOLID232 (Current-based Electric Element) elements were utilized for the halo current simulation, while SOLID237 (Electromagnetic Element) elements were used for the eddy current analysis. Both are 10-node tetrahedral elements.

3.3.2 Contact Definitions

For the purpose of an electromagnetic analysis, frictionless / frictional and bonded contacts are essentially the same, since we are only concerned with the current flow between the bodies. For the sake of simplicity, bonded contact was defined at all interfaces that are designed to be initially touching / closed contact.

The interface between the pins and pin holes was considered a closed contact for the purpose of EM analysis. There is 0.005” gap between the pin OD and the pin slot ID. However, once the pre-load and thermal loads are applied, this gap would most likely close. Since the halo current application follows the pre-load and thermal loads application, it is justified to consider this gap as closed.

3.3.3 Boundary Conditions and Loads

Figure 12 summarizes the boundary conditions, halo strike points and input currents. Table 1 lists the magnetic field components and dB/dt values. The values in the table, and the method of determining the halo current (as shown in Figure 12) was taken from NSTXU-CALC-11-08-00.

Table 1: Magnetic Field Inputs Summary

	Tile Dimensions [m]	**Final Magnetic Field Values [Tesla, T]**			**Field dB / dt [T/s]**		
Row	**Poloidal Width**	**Bx**	**By**	**Bz**	**dBx / dt**	**dBy / dt**	**dBz / dt**
7	0.142	-0.60	3.06	1.82	533	0	-1,915
8	0.130	0.45	3.06	2.23	-378	0	-2,469
9	0.142	0.46	3.06	2.15	-477	0	-2,430
10	0.142	0.62	3.06	1.45	-604	0	-1,697
11	0.142	0.51	3.06	0.89	-472	0	-1,082
12	0.142	-0.66	3.06	1.28	587	0	-1,613
13	0.142	-0.60	3.06	2.00	552	0	-2,508
14	0.142	0.16	3.06	2.10	-123	0	-2,698

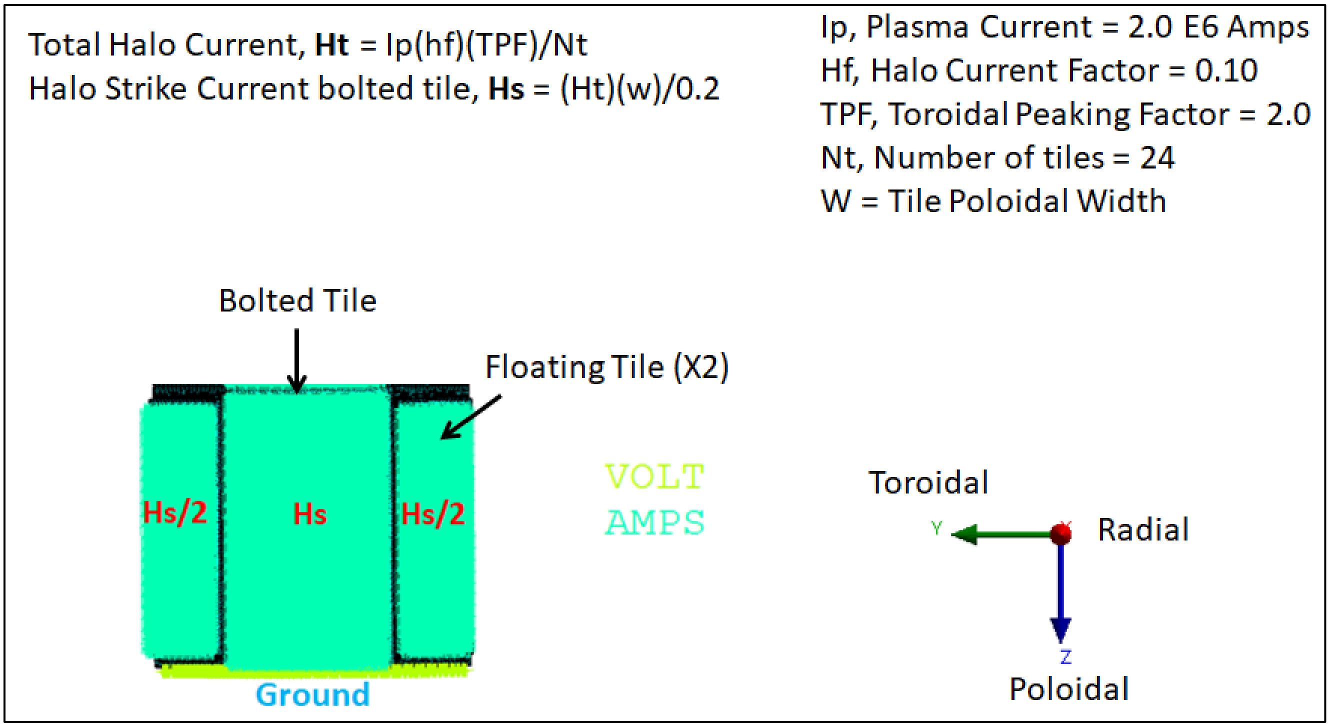

Figure 12: Boundary Conditions, Loads, and Halo Current Calculation

3.3.4 Results

Table 2: Electromagnetic Loads Summary

	Bolted Tile Halo Loads [N]			Floating Tile Halo Loads [N]			Bolted Tile Eddy Moments [NM]			Floating Tile Eddy Moments [NM]		
Row	**Fx**	**Fy**	**Fz**	**Fx**	**Fy**	**Fz**	**Mx**	**My**	**Mz**	**Mx**	**My**	**Mz**
7	-323	258	-537	-443	274	-600	-0.10	-4.38	7.33	-0.55	**-4.71**	7.74
8	-295	400	-492	-406	455	-549	**-0.12**	4.02	-5.50	**-0.67**	4.33	-5.81
9	**-323**	**424**	**-537**	**-443**	**483**	**-600**	-0.12	3.96	-5.60	-0.65	4.17	-5.81
10	-323	318	-537	-443	368	-600	0.00	3.60	-7.60	-0.44	3.88	**-8.00**
11	-323	208	-537	-442	244	-600	0.00	1.82	-6.23	-0.27	1.96	-6.57
12	-323	157	-537	-443	160	-600	0.00	-3.39	**8.06**	-0.39	-3.64	8.51
13	-323	289	-537	-443	309	-600	-0.10	**-4.81**	7.33	-0.61	-5.17	7.74
14	-323	384	-537	-442	432	-600	-0.12	1.35	-1.96	-0.64	1.45	-2.06

The electromagnetic load reaction results are summarized in Table 2. The Halo force values are sums of all nodal forces in the tiles. These are useful for determining which row experiences the highest forces. As highlighted in the table, row 9 undergoes the highest forces. The eddy moments are minute but measureable, and are also highlighted. Positive X-direction is away from the center stack casing.

The nodal force information (node coordinates, Fx, Fy, Fz, node volume, body force densities) was output to a text file. The body force densities are defined as nodal force / nodal volume, and may be imported to a Multiphysics model to study the effect of combined loading (structural, thermal and electromagnetic).

Figure 13 shows the current density within the assembly. The majority of current entering through the tiles discharges through the ground specified on the casing surface. This is indicated by a large region of grey contours in the figure.

The nodal forces are also concentrated close to the ground, and are in the negative x direction – i.e. the tile is being pushed on to the center stack casing.

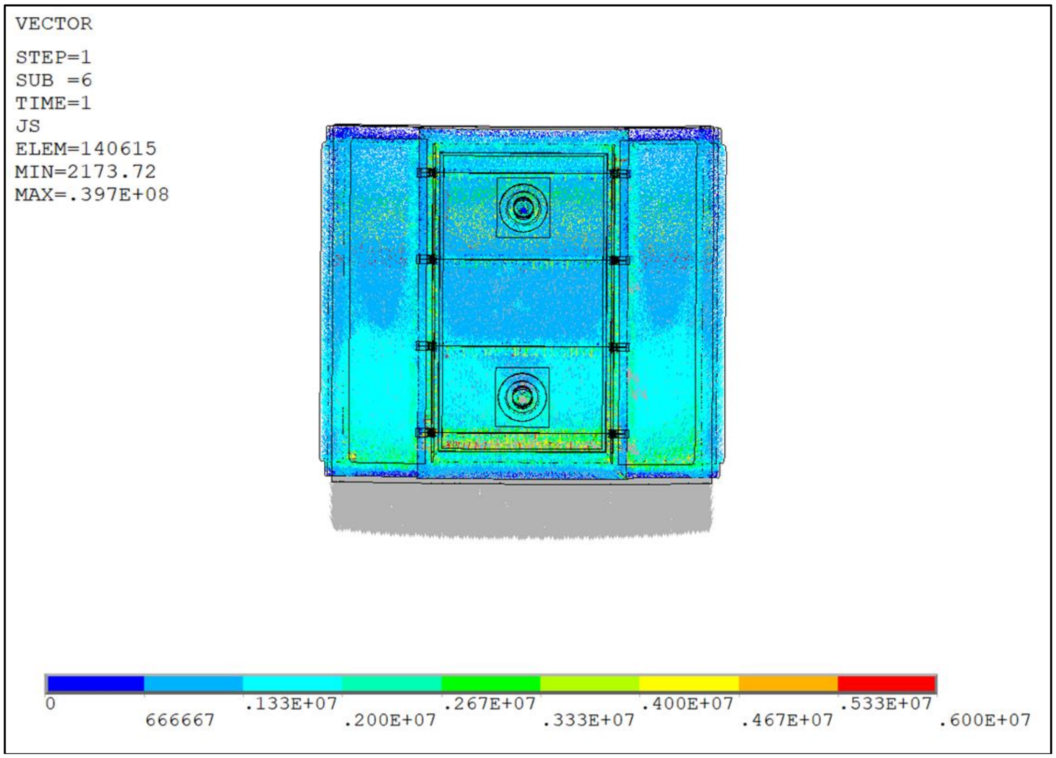

Figure 13: Total Current Density, Row 9

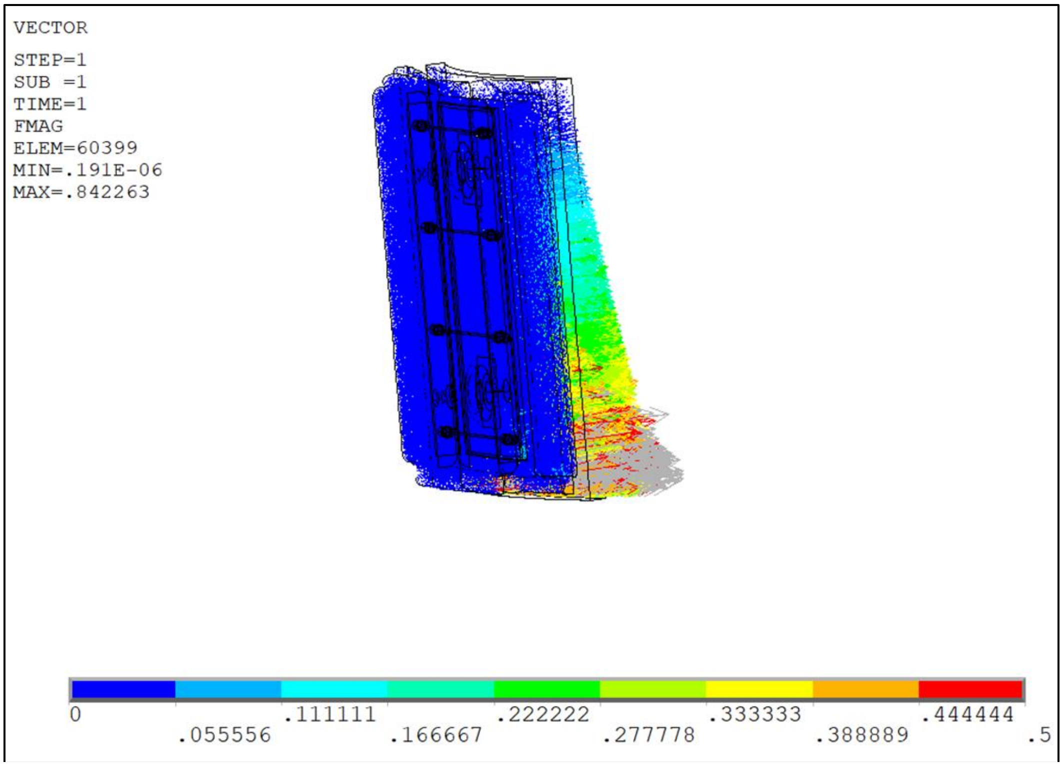

Figure 14: Nodal Magnetic Forces, Row 9

3.4 Structural Analysis

The results from the thermal and electromagnetic analyses were imported into a structural model as input loads. The following procedure was followed:

1) Apply 6.5 ft-lb (5,555 N) preload torque to weld nuts. This value was determined thru testing. See reference XYZ.

2) Import temperature distribution from thermal model. Based on established internal guidelines (See reference XYZ), the temperature distribution spanning 60 seconds, starting at the end of the first halo pulse is imported. The structural pre-processor converts these temperatures to displacement loads based on material CTEs.

3) Based on the results of the EM analysis, import body force densities for row 9. Body force density is imported for every node in the tile and bracket, and is defined by nodal force / nodal volume (N / M^3).

4) Simultaneously with step 3, apply eddy moments to all external faces of the tiles.

5) Determine relevant stresses, displacements, strains and load reactions for the assembly.

6) Compare results with established allowable limits / testing results.

3.4.1 FE Mesh

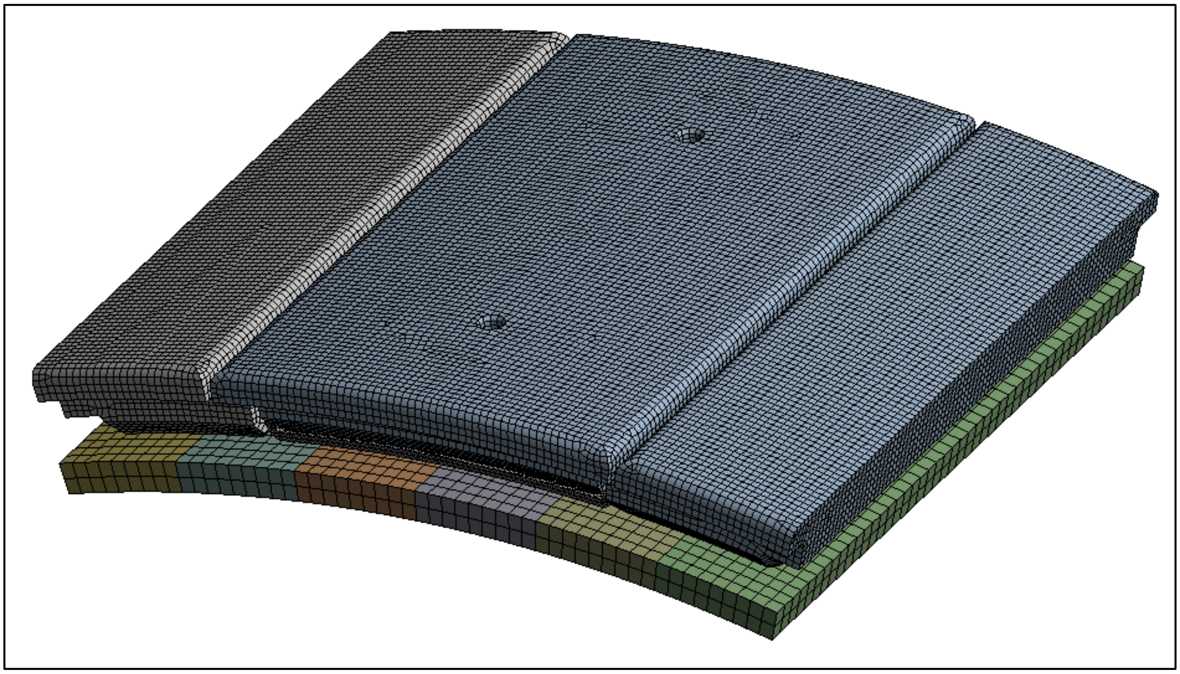

Figure 15: Structural Model Mesh

3.4.2 Contact Definitions

The contact definitions were identical to the definitions for the thermal model. See section 3.2.2.

3.4.3 Boundary Conditions and Loads

1) Frictionless supports were assigned to casing cut surfaces.

2) The cut surfaces on the two floating tile halves were coupled in all DOF (translations and rotations in X, Y, and Z axes).

3) Preload was applied to the weld studs.

4) Temperature distribution from the thermal model was imported.

5) Body force densities for the tiles and bracket were imported from the EM analysis.

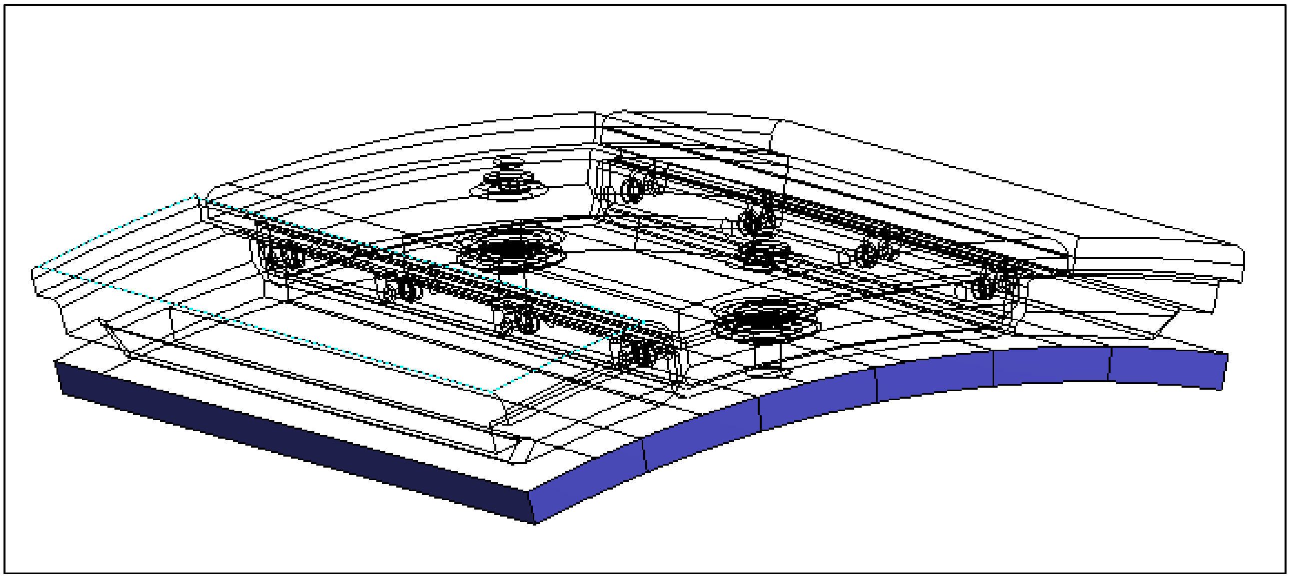

Figure 16: Casing Surfaces Frictionless Support

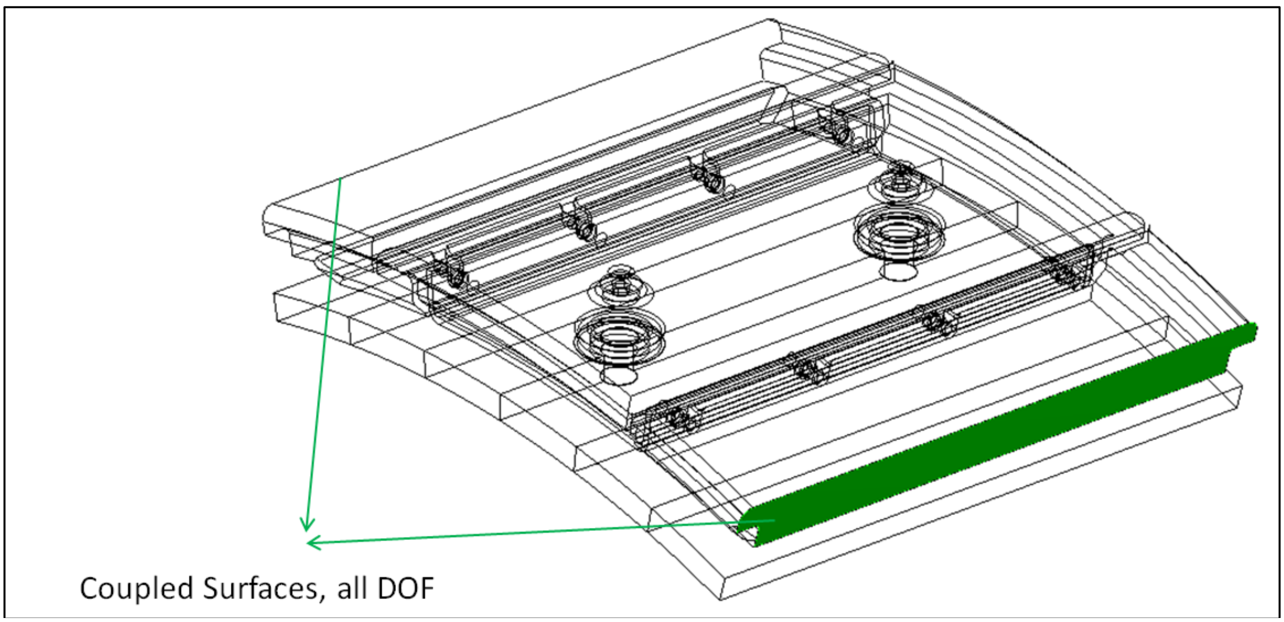

Figure 17: Coupled Surfaces

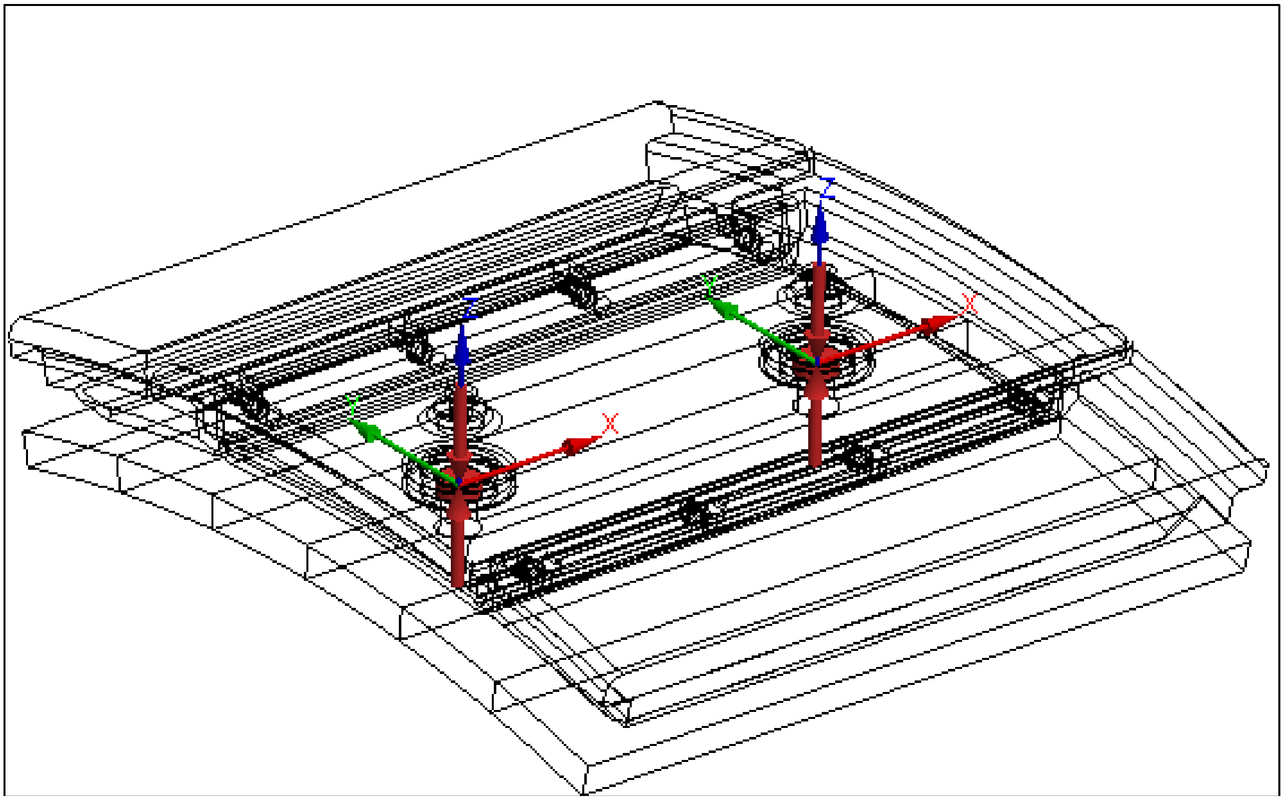

Figure 18: 5,555 N Pretension (6.5 ft-lbf torque)

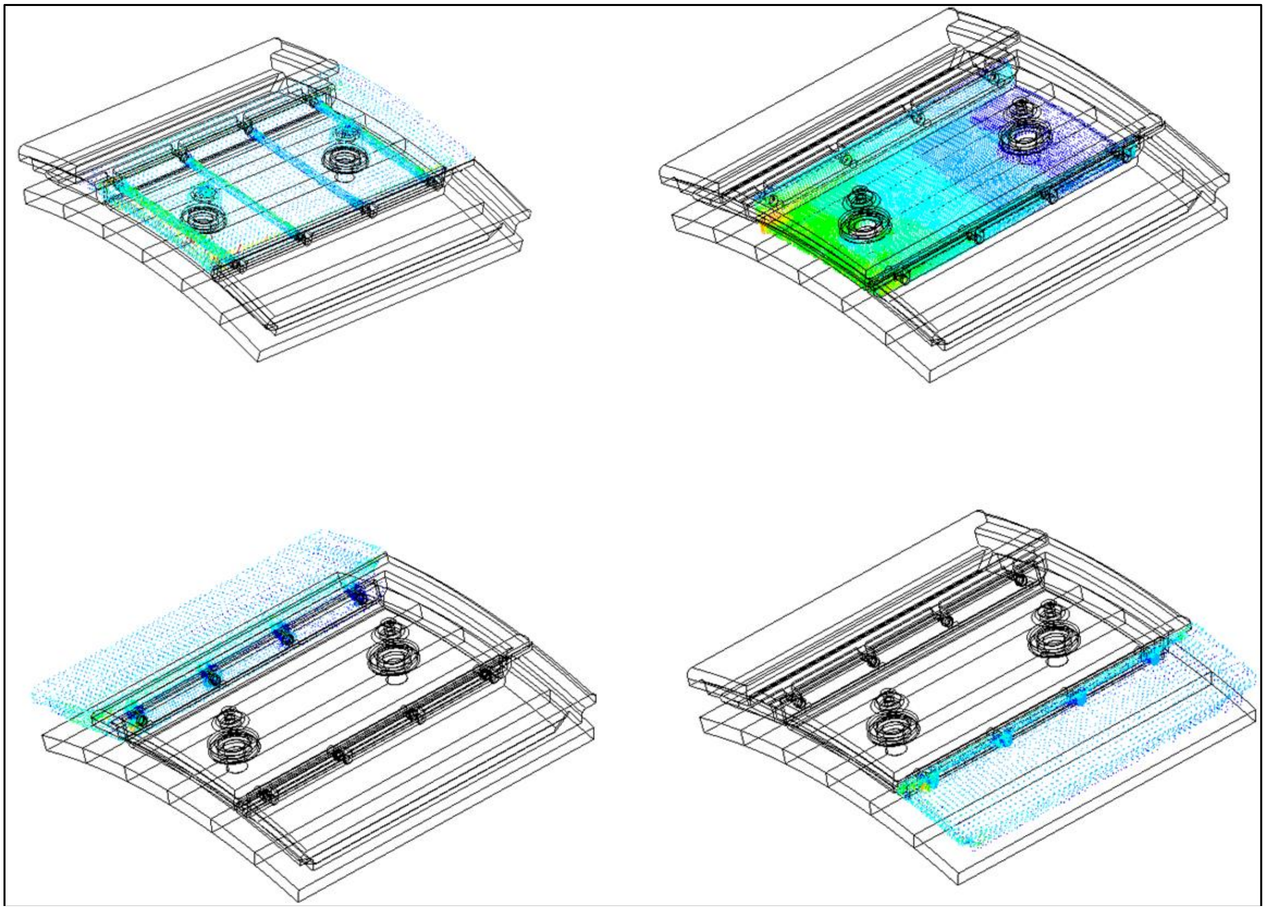

Figure 19: Body Force Densities

3.4.4 Structural Acceptance Criteria

The NSTX structural design requirement outlines the allowable stress limits. These stress limits are based on multiple factors which are specified in the NSTX requirements document.

Table 3: Design Stress, Sm [MPa] – Metallic Components

Component	Metal Component Type	Material	YS	TS	2/3 YS	1/2 TS	Min (2/3 YS, 1/2 TS)
Bracket	Conducting	Alloy 718	1,071	1,369	714	685	685
Weld Nut	Steel / Bolting	Grade 660 SS	671	939	447	469	447
Washer*	Steel / Bolting	Alloy 718	1,071	1,369	714	685	685
Weld Stud	Steel / Bolting	Alloy 625	397	782	264	391	264
Pins	Conducting	Alloy 625	397	782	264	391	264

***The analysis was run with 316LSS material assigned to the washer. However, the results showed that a higher strength material (Alloy 718) must be utilized. The results will be presented based on Alloy 718 allowable stresses.**

Table 3 specifies the design stresses (Sm) for the metallic components (highlighted cells). The allowable stress limits are based on the design stresses and are as follows:

- General Primary Membrane Stress < 1.0*K*Sm
- Local Primary Membrane Stress < 1.50*K*Sm
- Primary Membrane plus Bending Stress < 1.5*K*Sm
- Total Primary plus Secondary Stress < 3.0*K*Sm

Where Sm is the design stress and K is dependent on the level of service condition. For this analysis k is 1.0 (normal operating conditions).

Table 4: PFC Allowable Stress Limits [MPa]

Component	Material	Flexural Strength	Compressive Strength	½*FS	½*CS
Bolted Tile	PocoTM	59	110	29.5	55
Floating Tile	Graphite SGL R6510	60	130	30	65

Table 4 lists the material strengths and the maximum allowable tensile and compressive stresses for the tiles.

3.4.5 Results

The structural analysis can be divided into four phases:

1) Preload application (Primary Stress)
2) End of first halo pulse temperature application (Primary + Secondary Stress)
3) 60 Seconds after end of first halo pulse (Primary + Secondary Stress)
4) Electromagnetic loads application (Primary + Secondary Stress)

The types of stresses induced during each phase are categorized as shown in the parenthesis.

3.4.5.1 Bracket Results

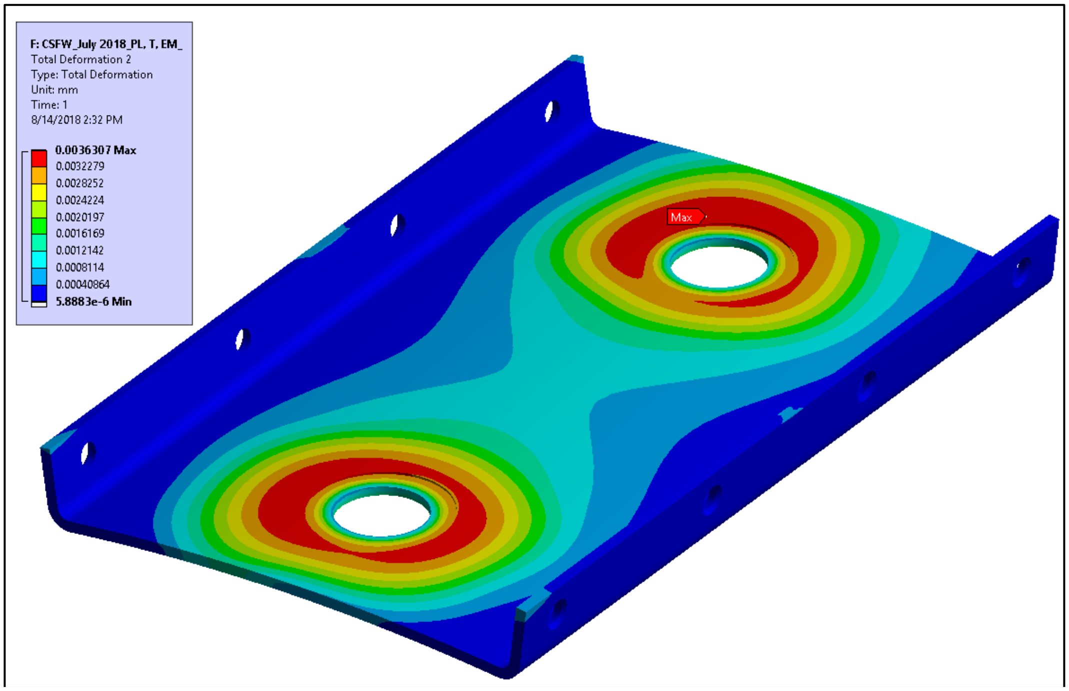

Figure 20: Bracket Total Deformation at Preload

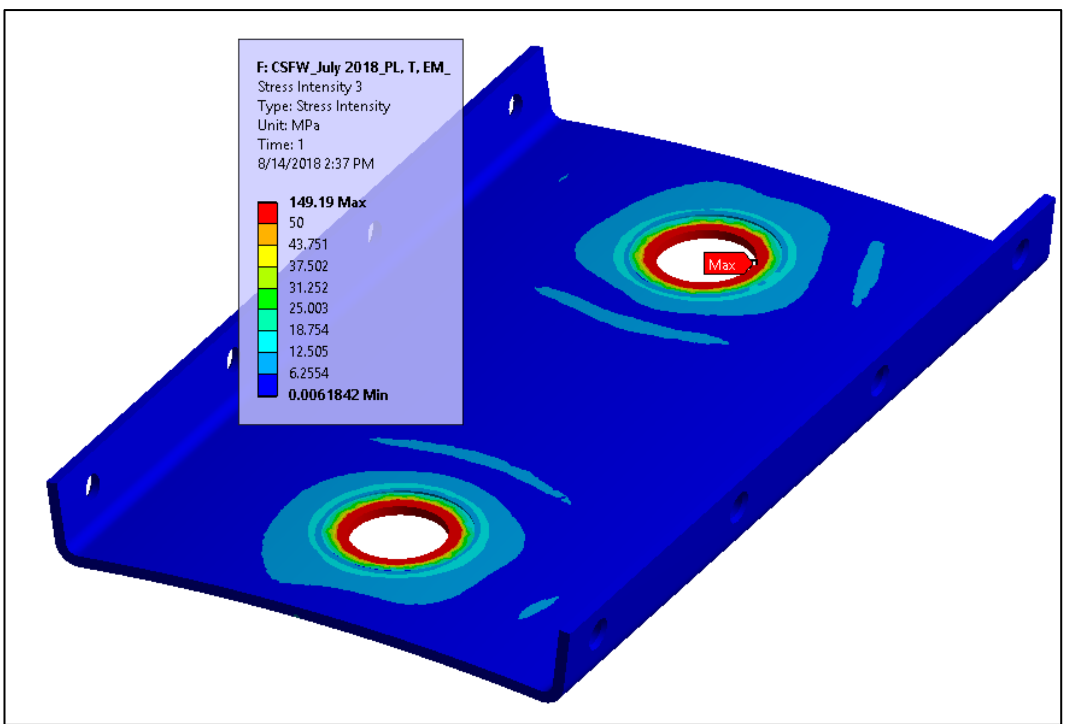

Figure 21: Bracket Stress Intensity at Preload

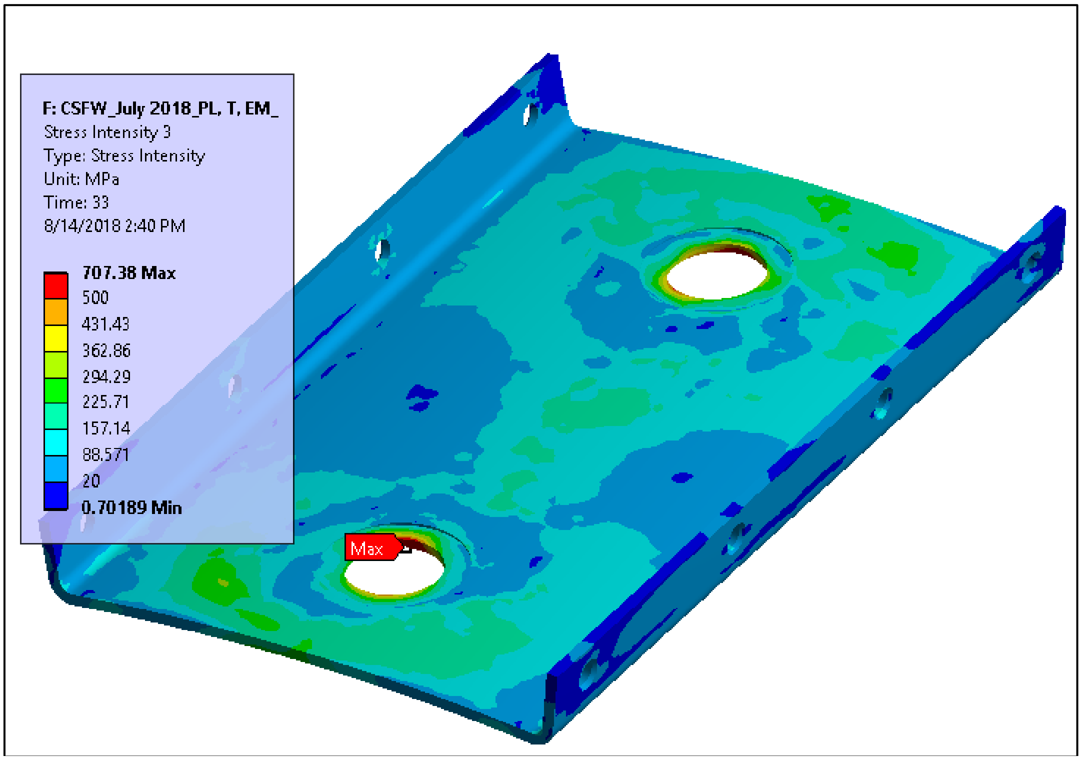

Figure 22: Bracket Maximum Stress Intensity (Preload plus Temperature)

The mesh in the area around the high stresses was refined via sub-modeling before performing stress linearization to determine the appropriate membrane and bending stresses.

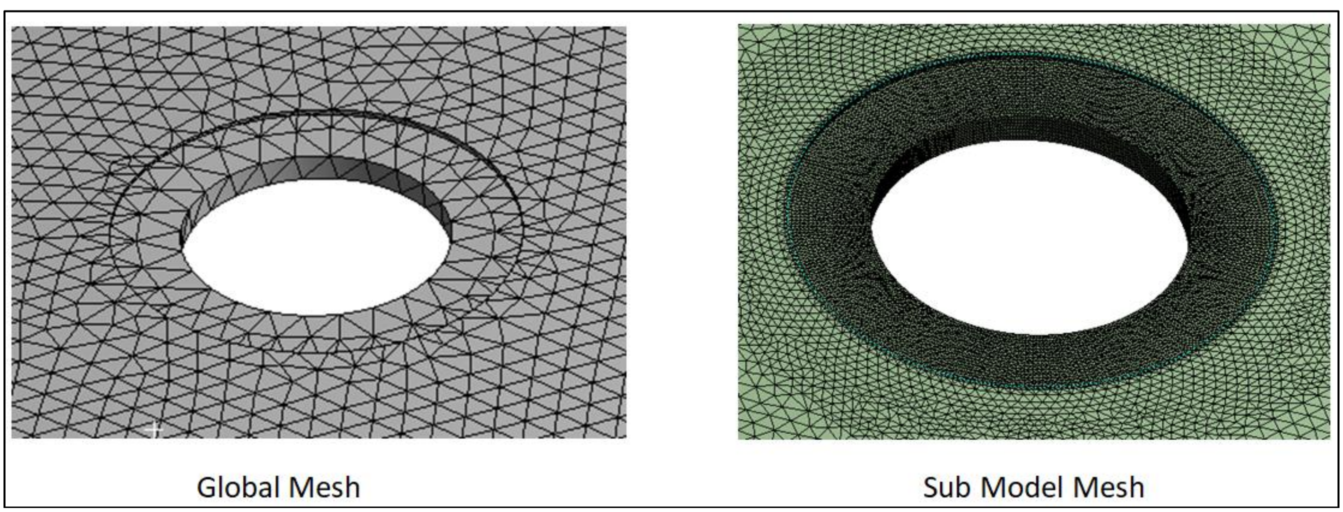

Figure 23: Bracket Mesh Comparison

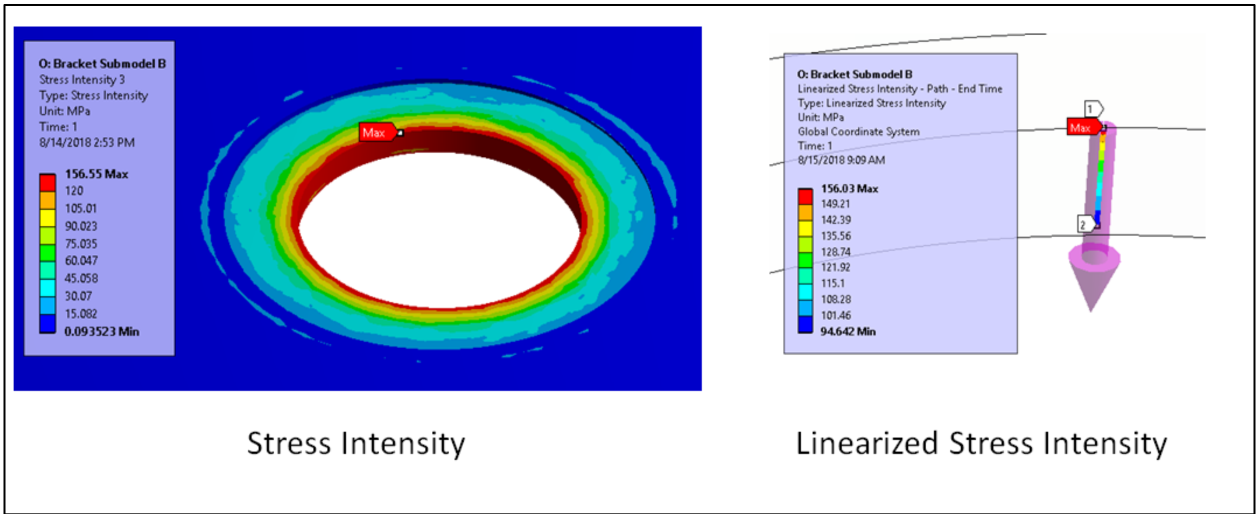

Figure 24: Bracket Sub Model Stress Intensity at Preload

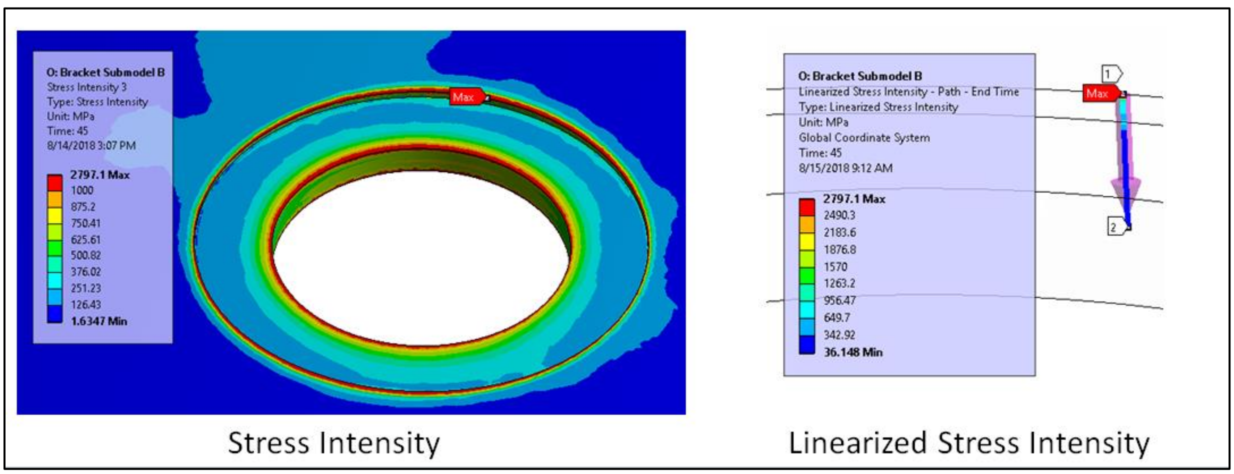

Figure 25: Bracket Maximum Sub Model Stress Intensity [44 seconds after halo pulse]

Table 5: Bracket Stress Intensity Results Summary [MPa]

Stress Type	**Load State**	**Observed**	**Maximum Allowable**	**Safety Factor**
General Primary Membrane Stress	Preload	121	1.0*1.0*714 = 714	0.17
Primary Membrane + Bending Stress	Preload	151	1.5*1.0*714 = 1,071	0.14
Total Primary + Secondary Stress	44 Seconds after Halo Pulse	474	3.0*1.0*714 = 2,142	0.22

3.4.5.2 Weld Nut Results

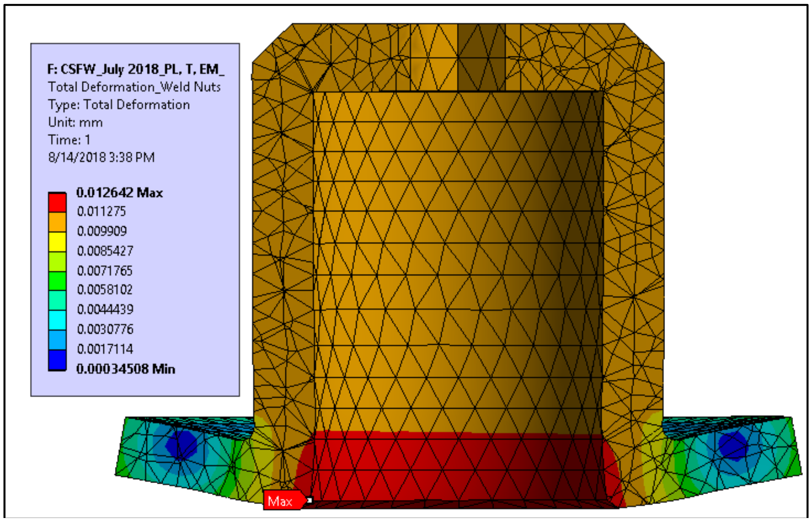

Figure 26: Weld Nut Total Deformation at Preload (X50 Scale)

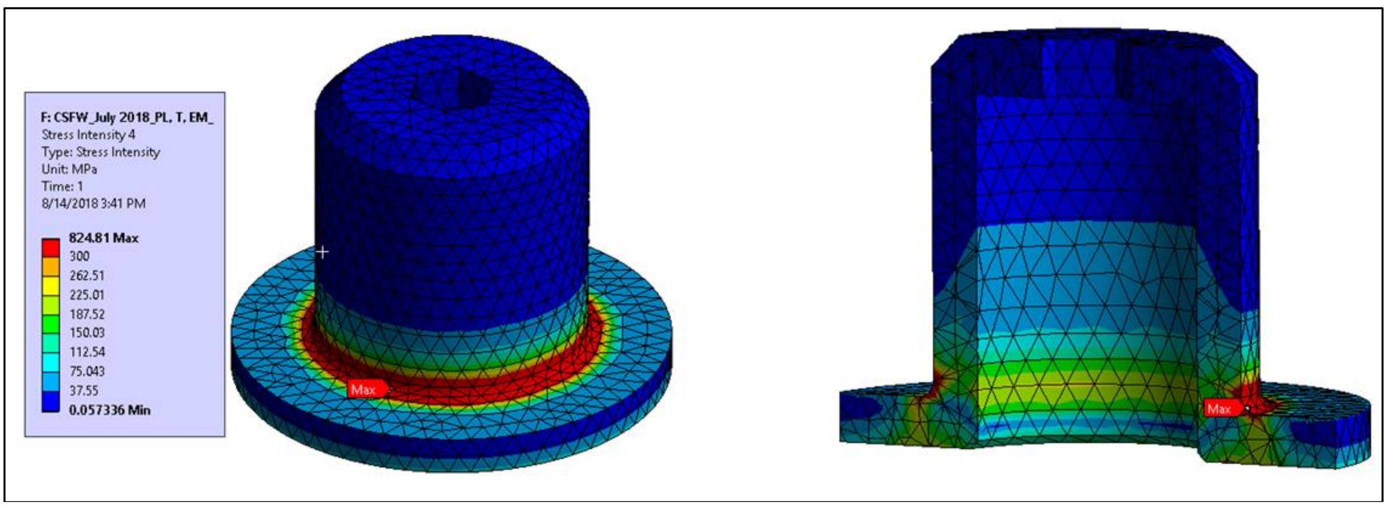

Figure 27: Weld Nut Stress Intensity at Preload

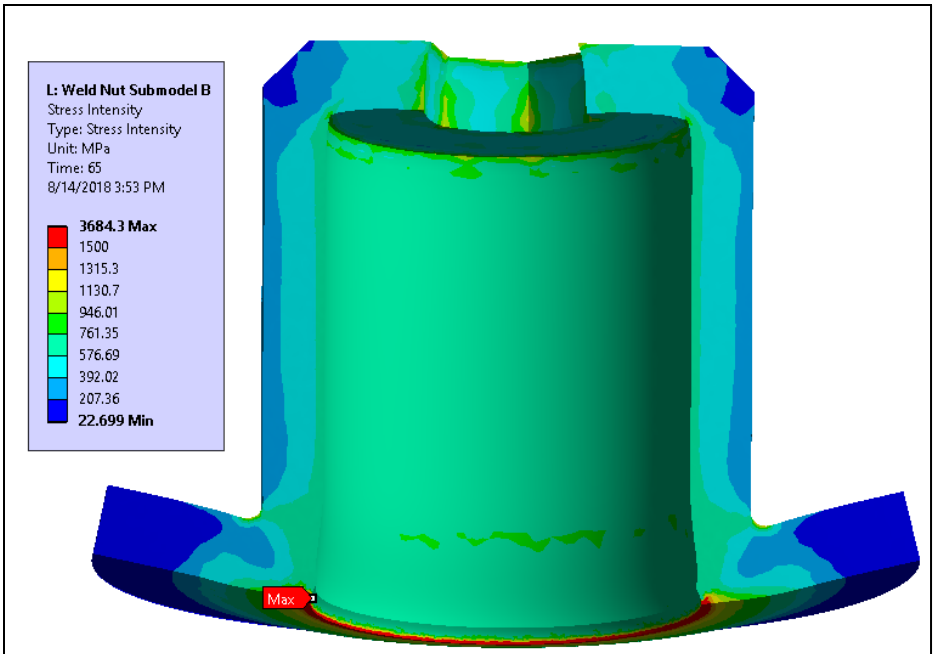

Figure 28: Weld Nut Maximum Stress Intensity (X50 Scale)

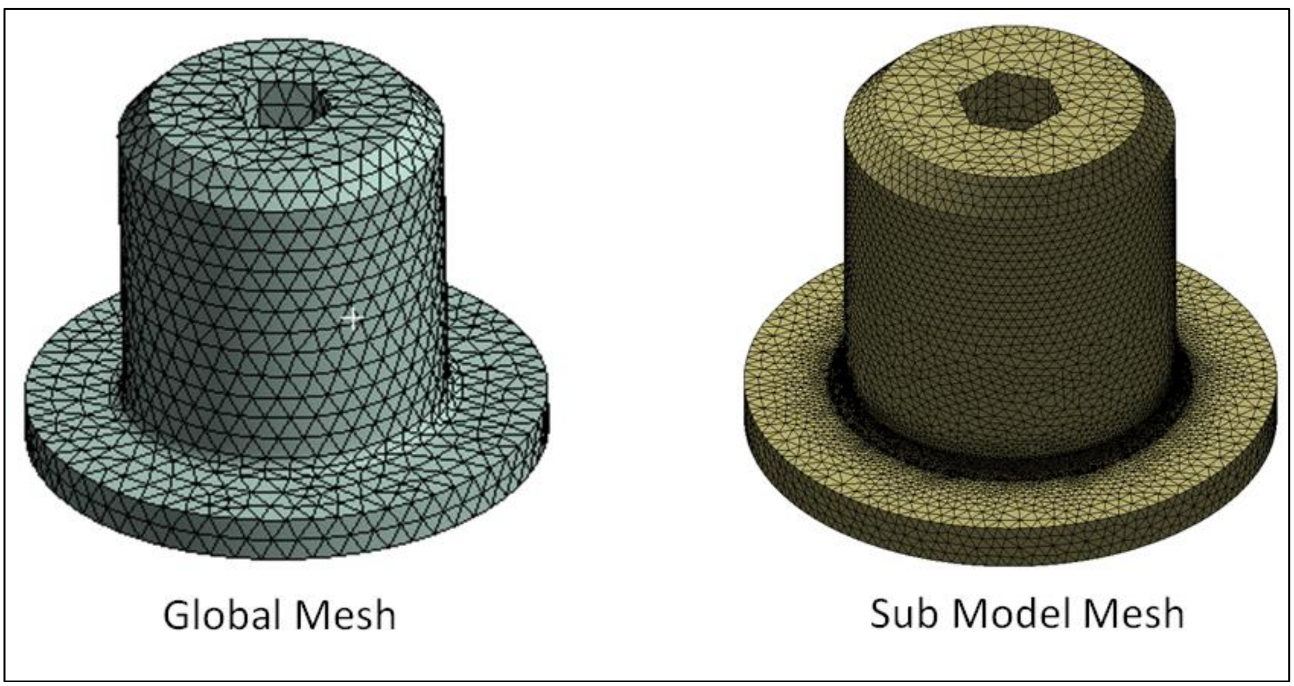

Figure 29: Weld Nut Mesh Comparison

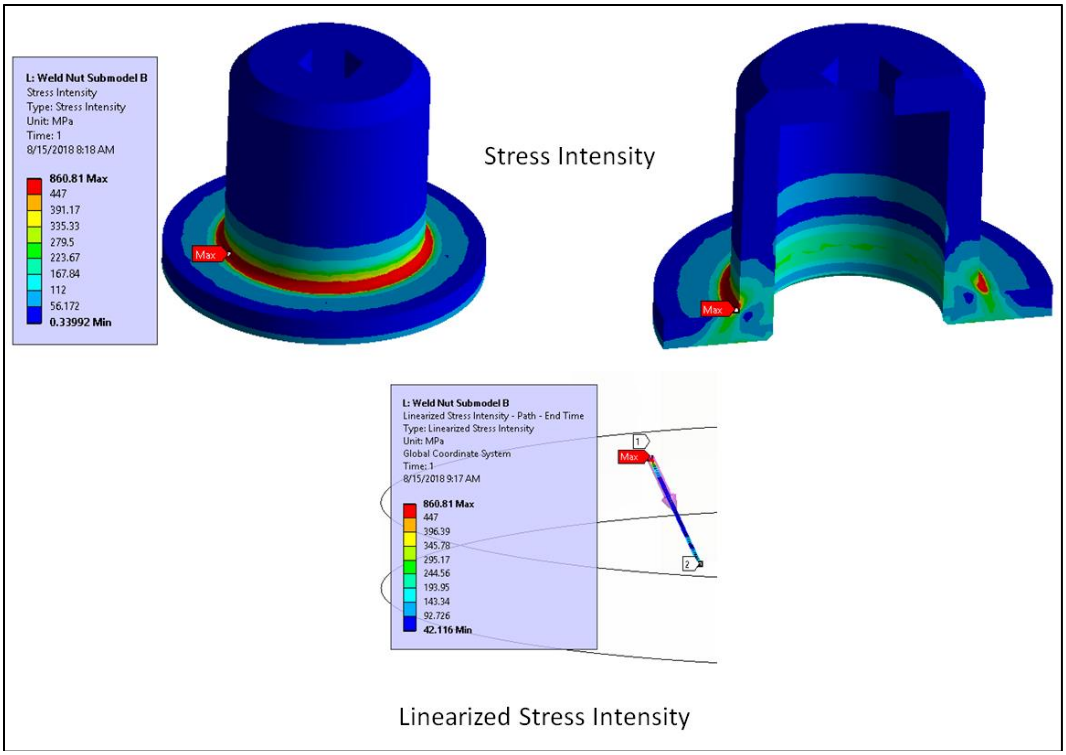

Figure 30: Weld Nut Sub Model Stress Intensity at Preload

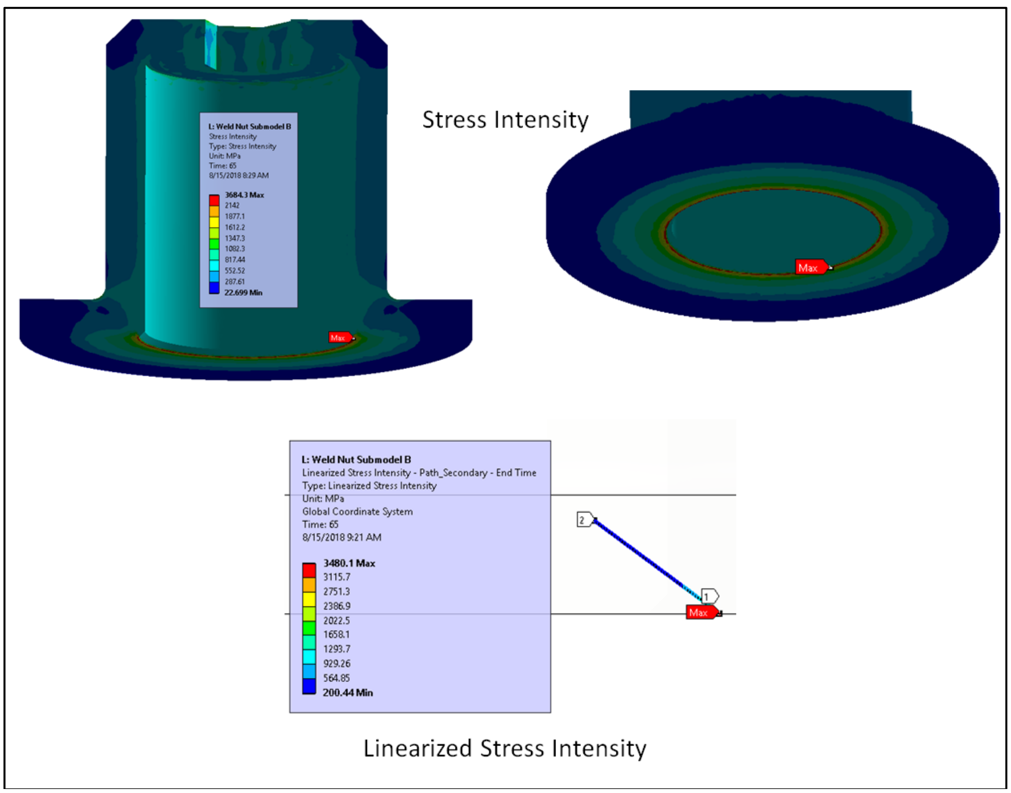

Figure 31: Weld Nut Sub Model Max. Stress Intensity [60 Seconds after halo pulse]

Table 6: Weld Nut Stress Intensity Results Summary [MPa]

Stress Type	**Load State**	**Observed**	**Maximum Allowable**	**Safety Factor**
General Primary Membrane Stress	Preload	68	1.0*1.0*447 = 447	0.15
Primary Membrane + Bending Stress	Preload	180	1.5*1.0*447 = 670	0.27
Total Primary + Secondary Stress	60 Seconds after Halo Pulse	1,166	3.0*1.0*447 = 1,341	0.87

3.4.5.3 Washer Results

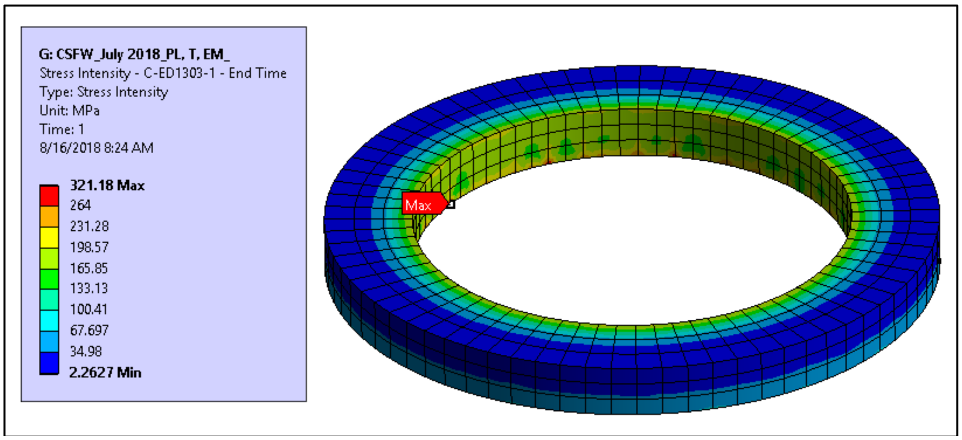

Figure 32: Washer Stress Intensity at Preload

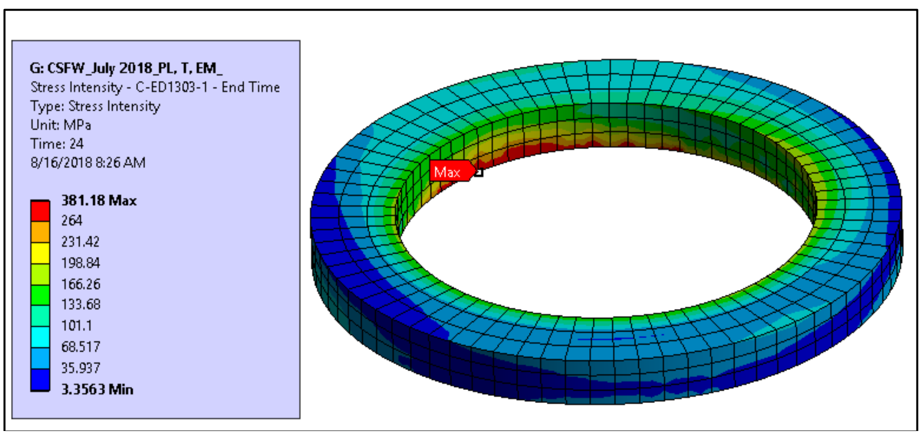

Figure 33: Washer Max. Stress Intensity

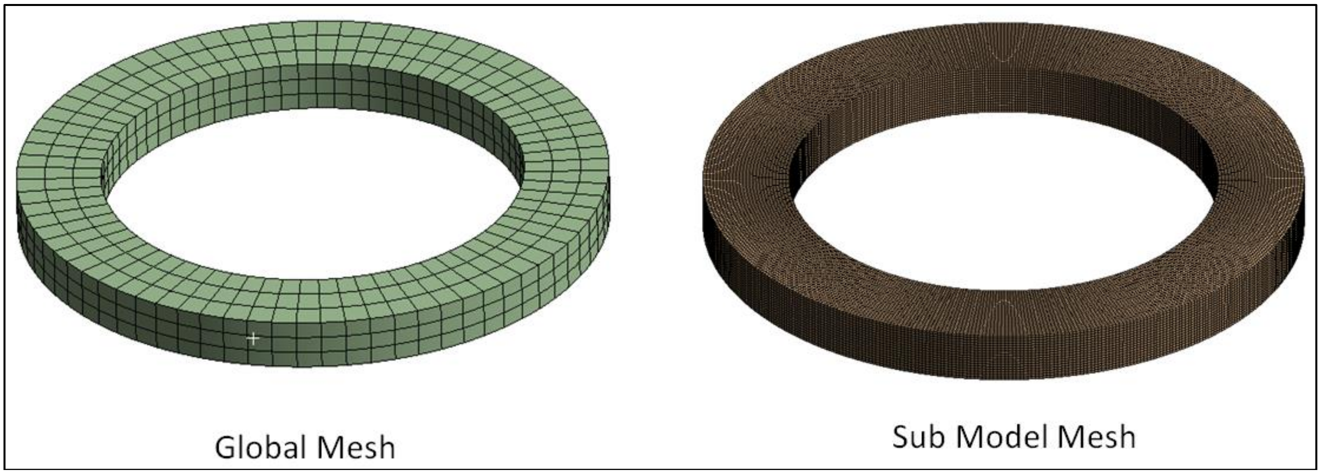

Figure 34: Washer Mesh Comparison

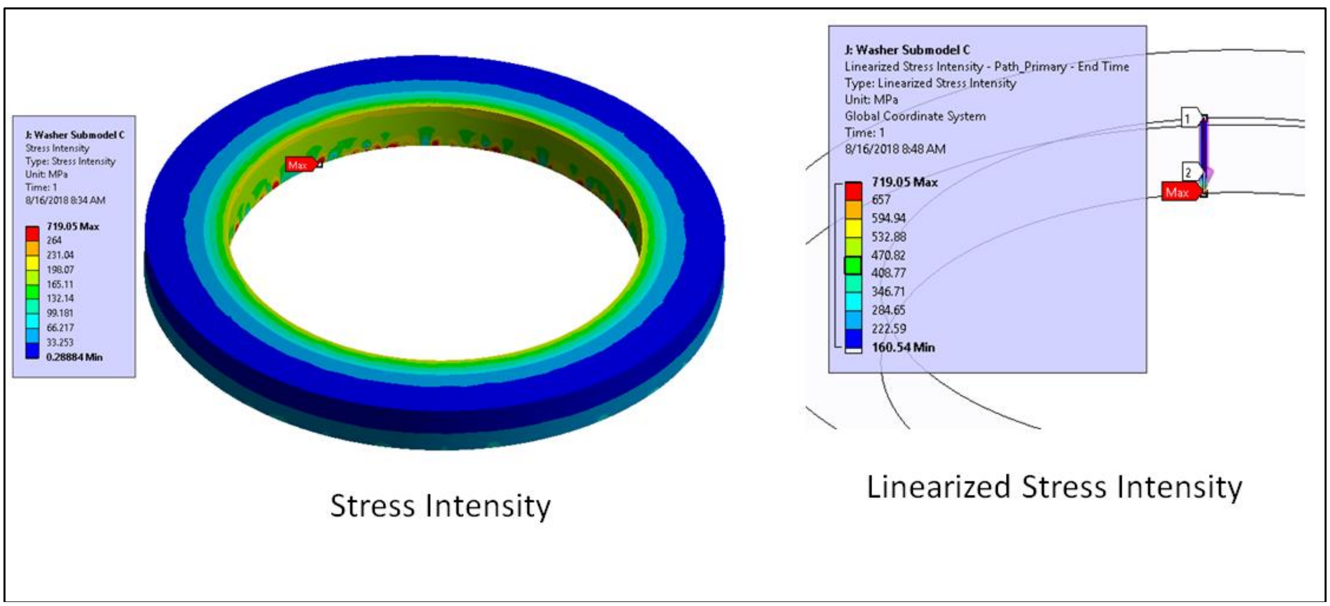

Figure 35: Washer Sub Model Linearized Stress Intensity at Preload

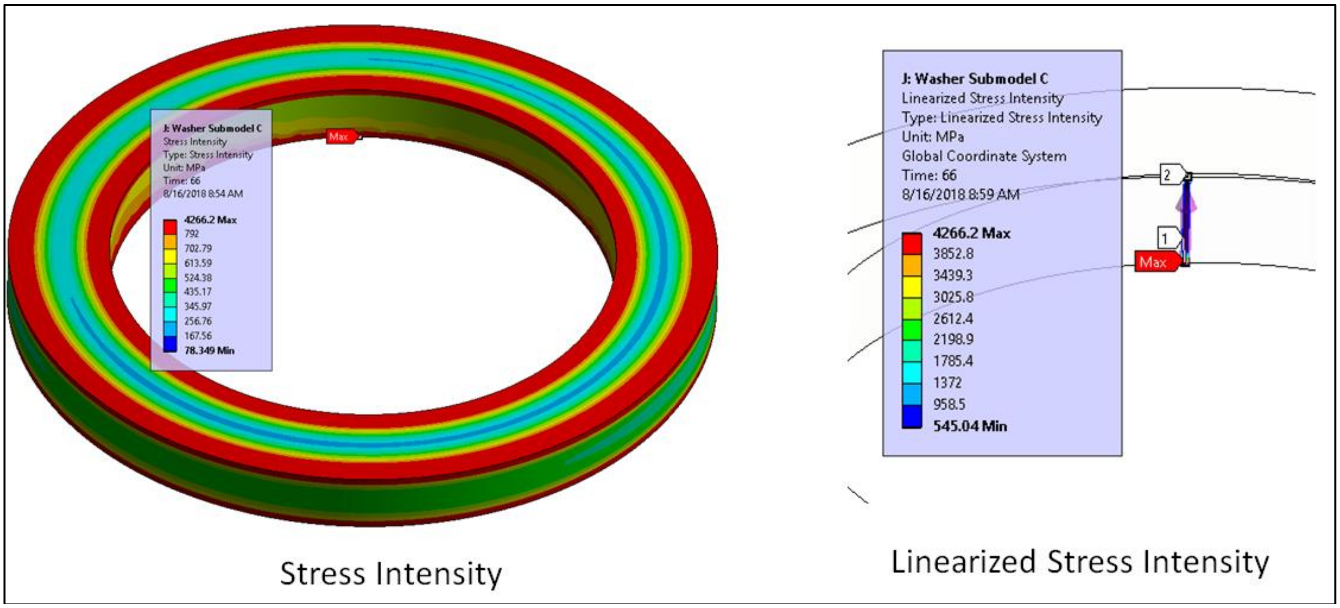

Figure 36: Washer Sub Model Maximum [EM loads] Stress Intensity

Table 7: Washer Stress Intensity Results Summary [MPa]

Stress Type	Load State	Observed	Maximum Allowable	Safety Factor
General Primary Membrane Stress	Preload	210	1.0*1.0*714 = 714	0.29
Primary Membrane + Bending Stress	Preload	368	1.5*1.0*714 = 1,071	0.34
Total Primary + Secondary Stress	EM Loads	938	3.0*1.0*714 = 2,142	0.44

3.4.5.4 Pin Stress Results

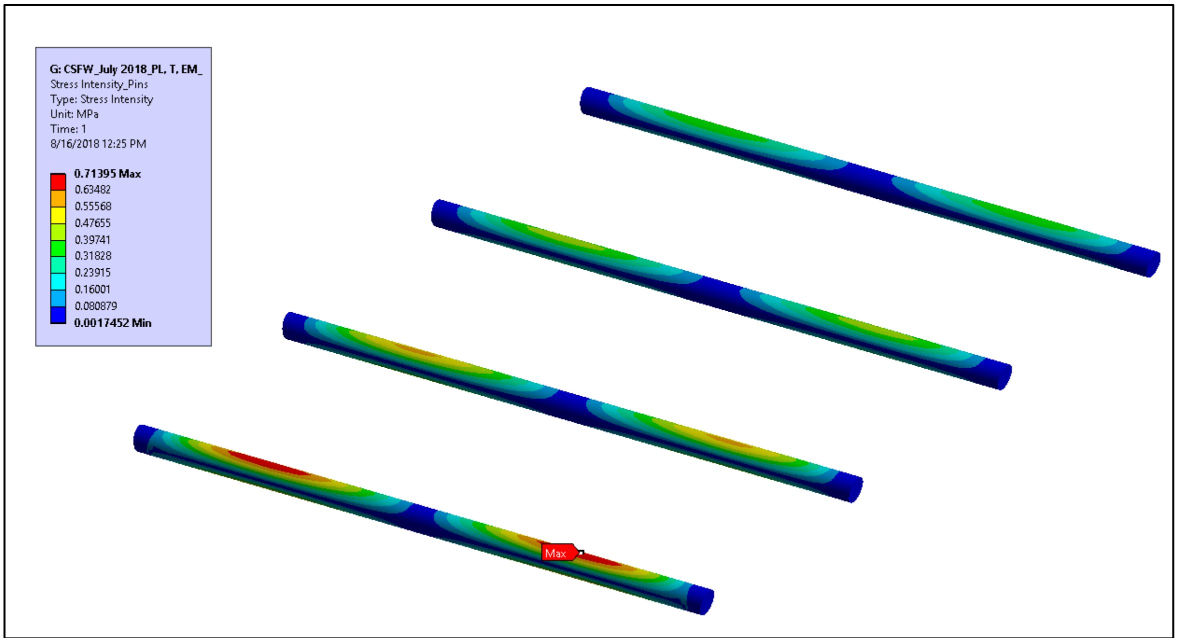

Figure 37: Pins Stress Intensity at Preload

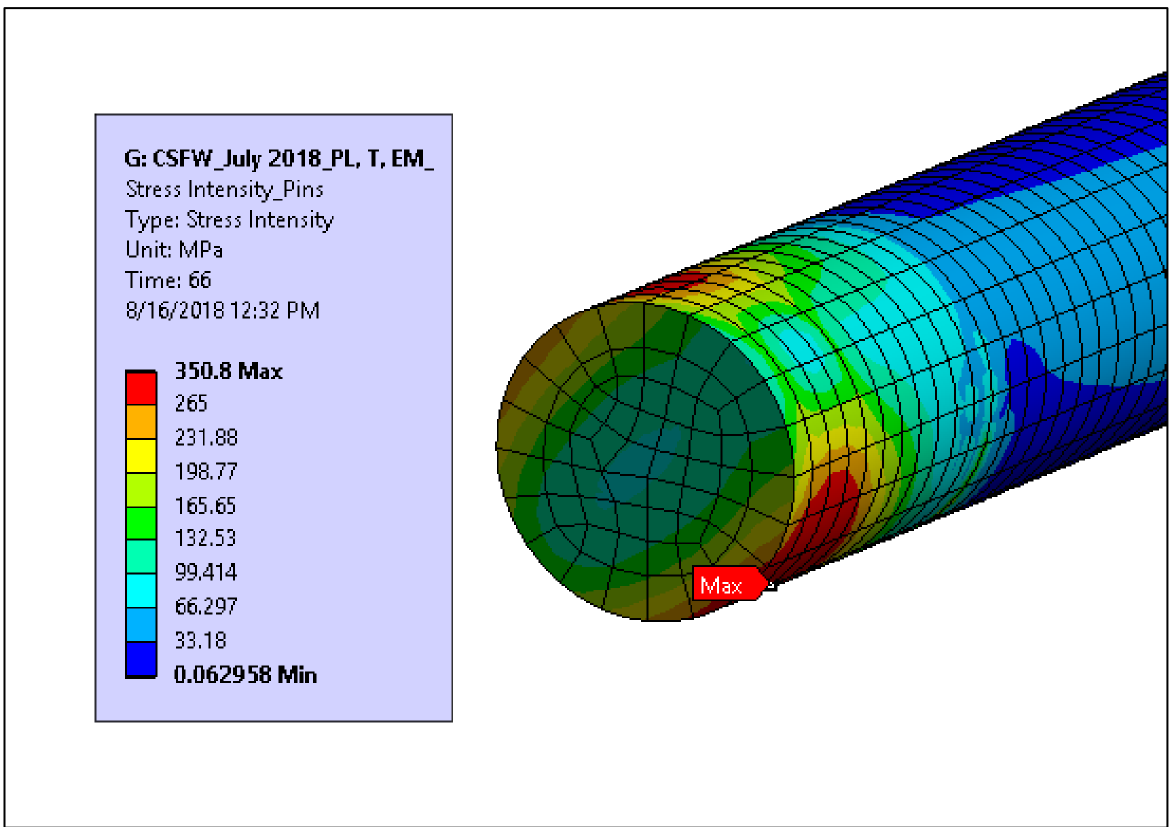

Figure 38: Pin Maximum Stress Intensity [EM Loads]

The primary stress intensity (at preload) is negligible as shown in Figure 37.

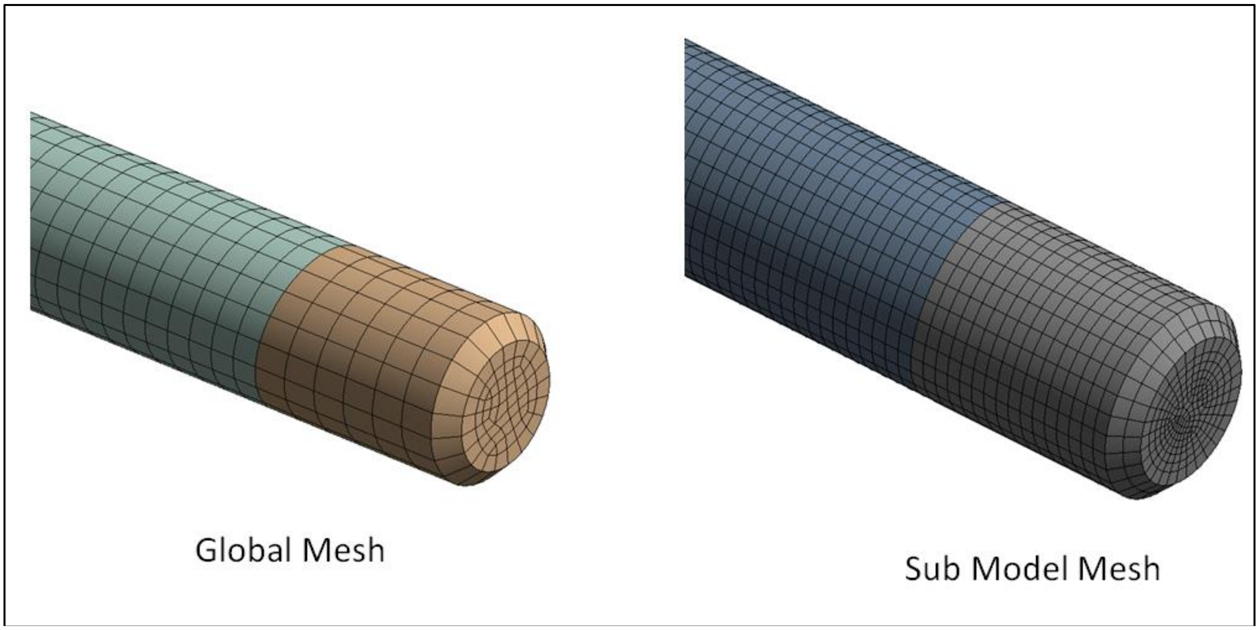

Figure 39: Pin Mesh Comparison

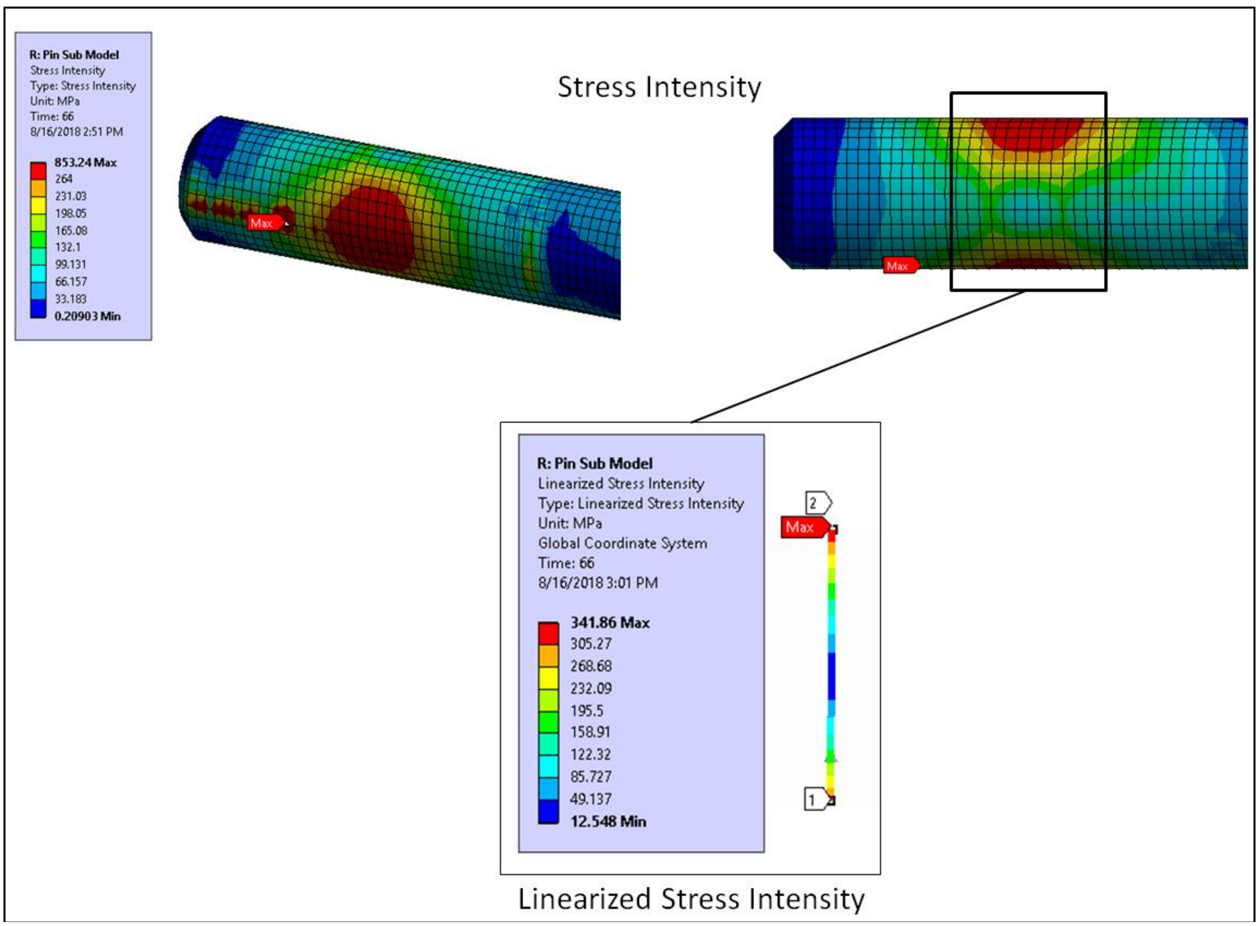

Figure 40: Pin Sub Model Maximum Stress Intensity [EM Load]

Table 8: Pin Stress Intensity Results Summary [MPa]

Stress Type	Load State	Observed	Maximum Allowable	Safety Factor
Total Primary + Secondary Stress	EM Loads	342	3.0*1.0*264 = 792	0.43

3.4.5.5 Bolted Tile Results

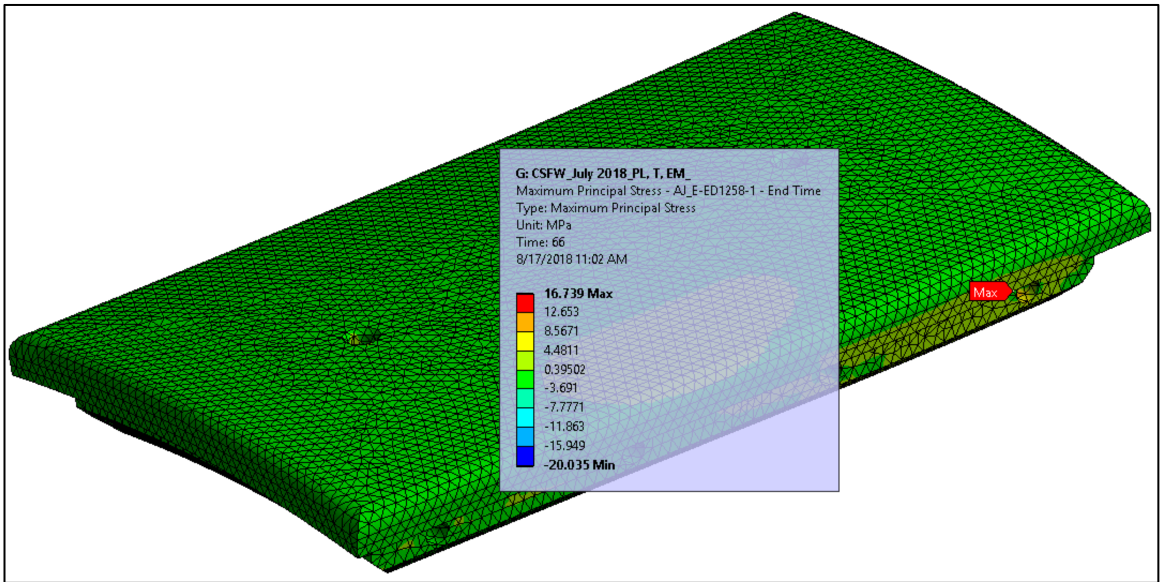

Figure 41: Bolted Tile Max. Principal Stress [EM Loads]

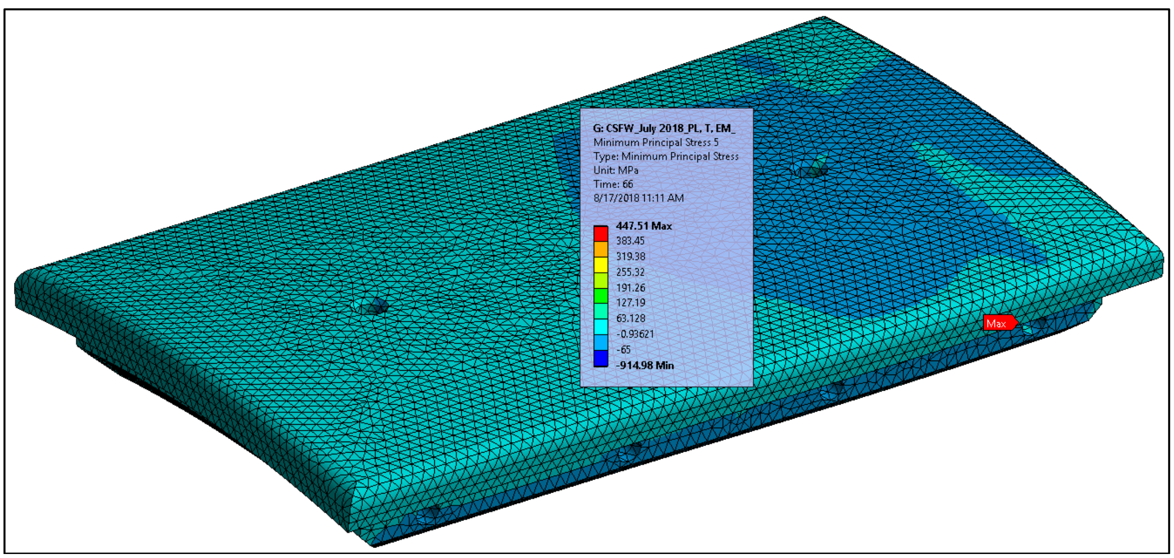

Figure 42: Bolted Tile Min. Principal Stress [EM Loads]

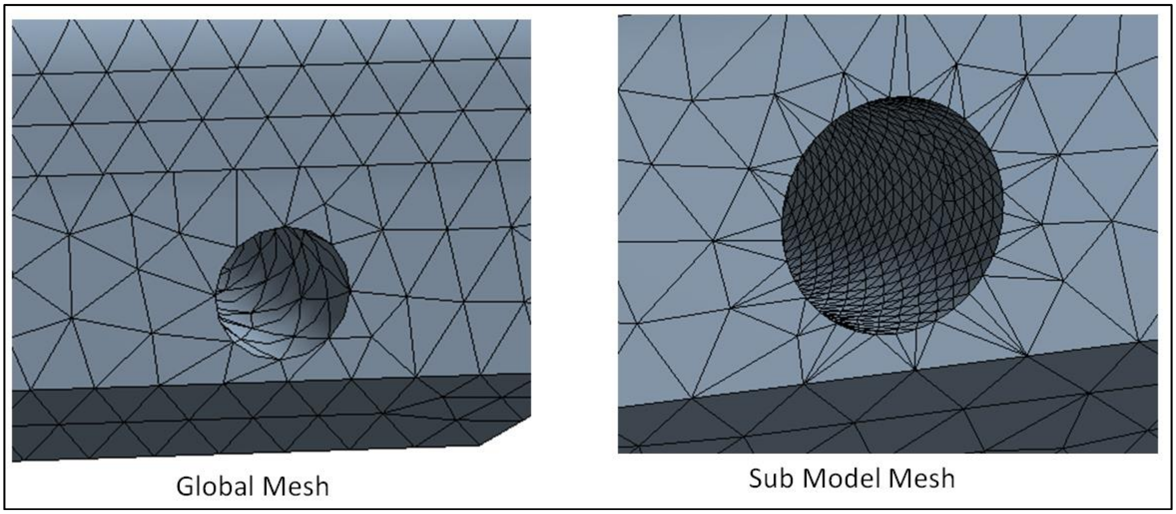

Figure 43: Bolted Tile Mesh Comparison

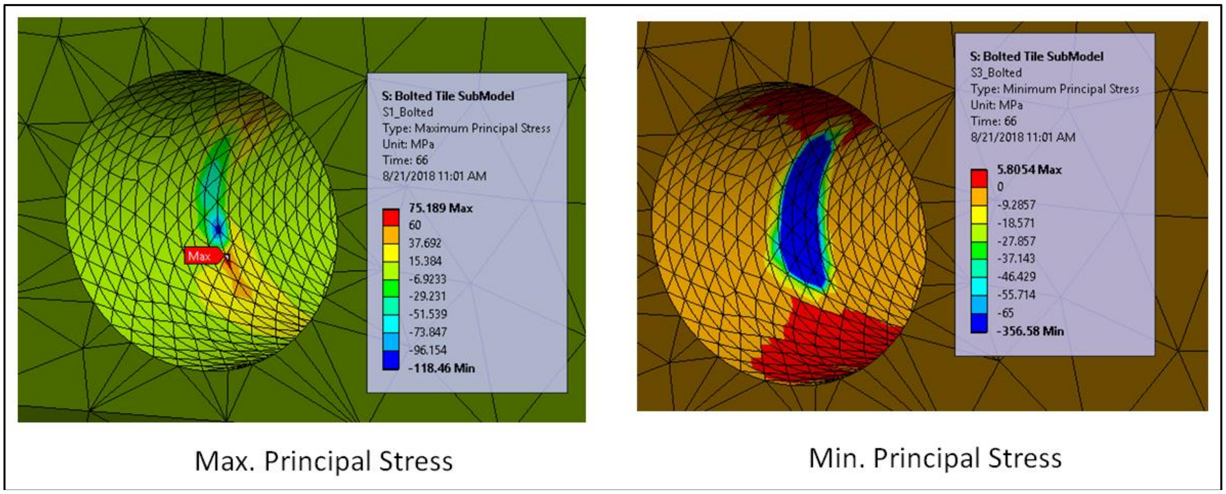

Figure 44: Bolted Tile Sub Model Max. and Min. Principal Stresses [EM Loads]

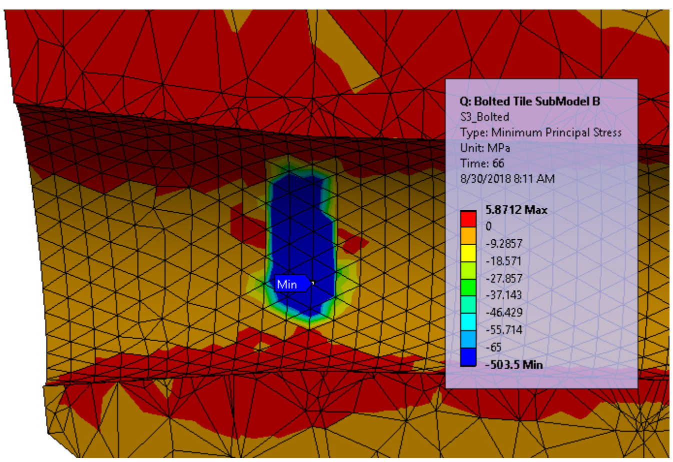

Figure 45: Bolted Tile Min. Principal Stress Cross Section [EM Loads]

The bulk stresses in the tile are well below the allowable stress limits. A region of significantly high compressive stress is observed inside the pin hole where the taper meets the straight bore (Figure 45). The pin OD makes contact with the taper as the tile assembly displaces under the influence of temperature and EM loads. A design change was made to alleviate this issue. The details and results of the design change are documented

3.4.5.6 Floating Tile Stress Results

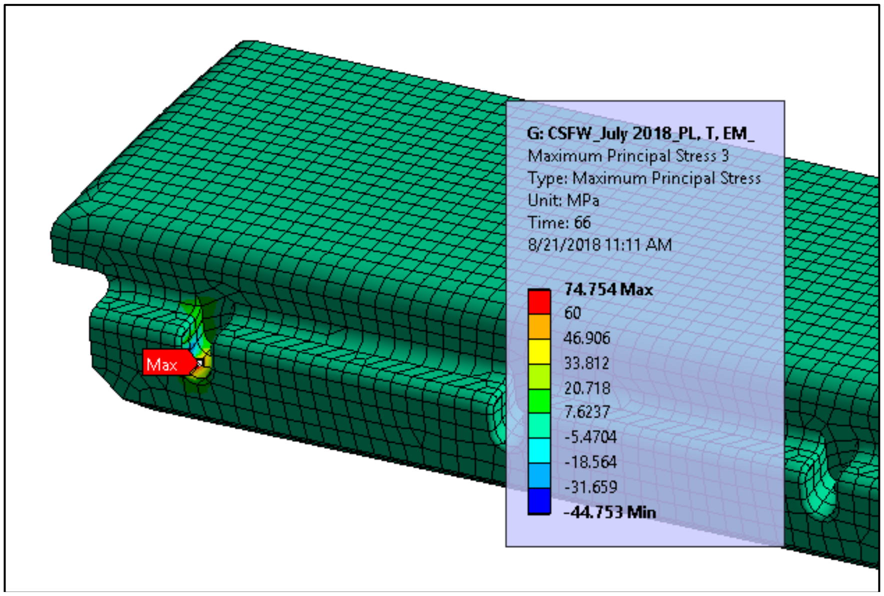

Figure 46: Floating Tile Max. Principal Stress [EM Loads]

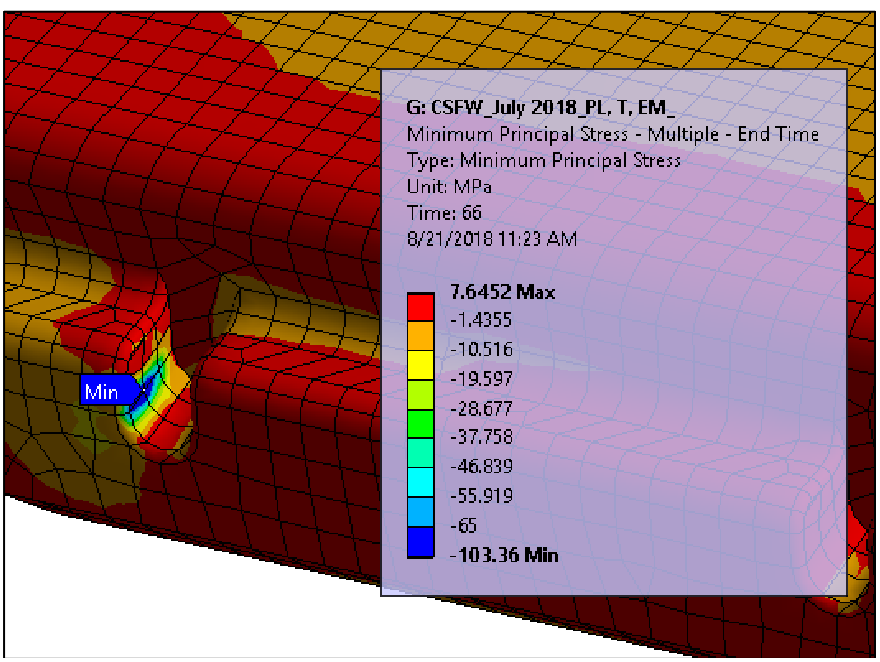

Figure 47: Floating Tile Min. Principal Stress [EM Loads]

The stresses on the floating tile pin slot surfaces follow a similar pattern to the ones observed for the bolted tile – A region of significantly high compressive stress at the pin – pin slot interface while the bulk tile stresses are well below the maximum allowable stresses. Performing a sub-modelling exercise was deemed unnecessary since it would only increase the stress values as observed with the bolted tile.

Based on the results of this analysis a few design changes were made to the bolted tile assembly. Four grafoil gaskets were utilized as cushioning between the pin and the bolted and floating tiles surfaces. This results in significant reduction in the compressive stresses.

Refer to RPT XYZ for the details of the upgraded design.

3.4.5.7 Tile Redesign Submodel

In order to alleviate the high compressive stresses experienced by the tiles at the pin – tile interface protective grafoil was introduced into the design. A schematic of the updated design is shown in Figure 48

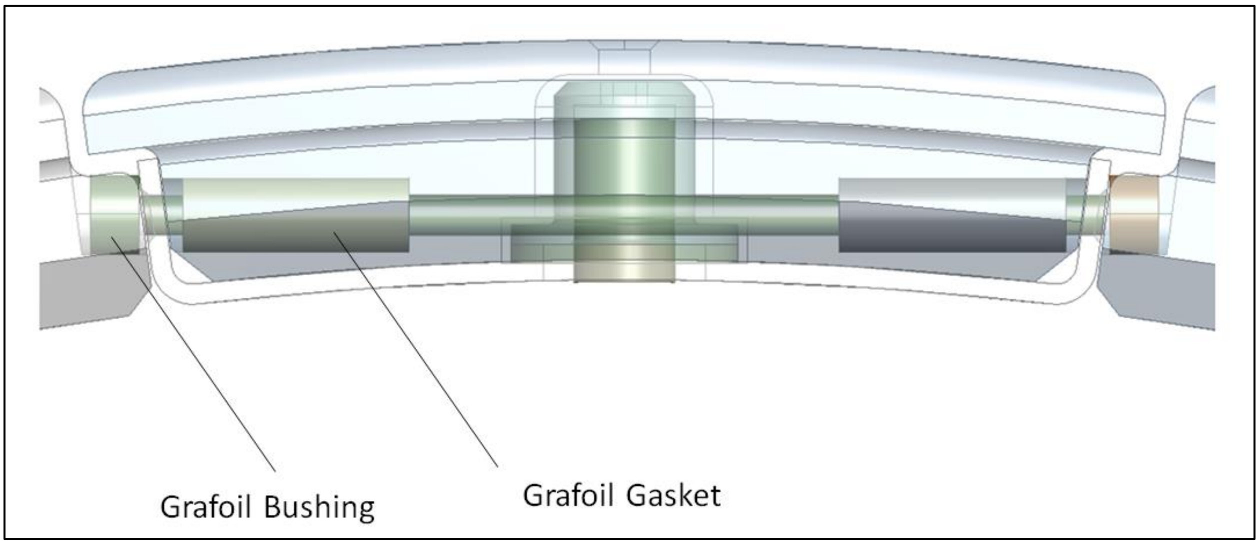

Figure 48: Tile Redesign

The intent is to protect the surface of the graphite tile. As an initial check, the existing geometry was modified as shown and a sub-modelling exercise was performed. For the initial run, the input loads for the sub-model were the same as the one's obtained from the original design.

Figure 49 and Figure 50 show the Min. Principal stresses in the bolted and floating tiles. The stresses have reduced significantly (-45 MPa bolted tile, -7 MPa floating tile) and are well below the maximum allowable limit of -55 MPa.

A full combined loading analysis will be performed to document the results for the updated tile design.

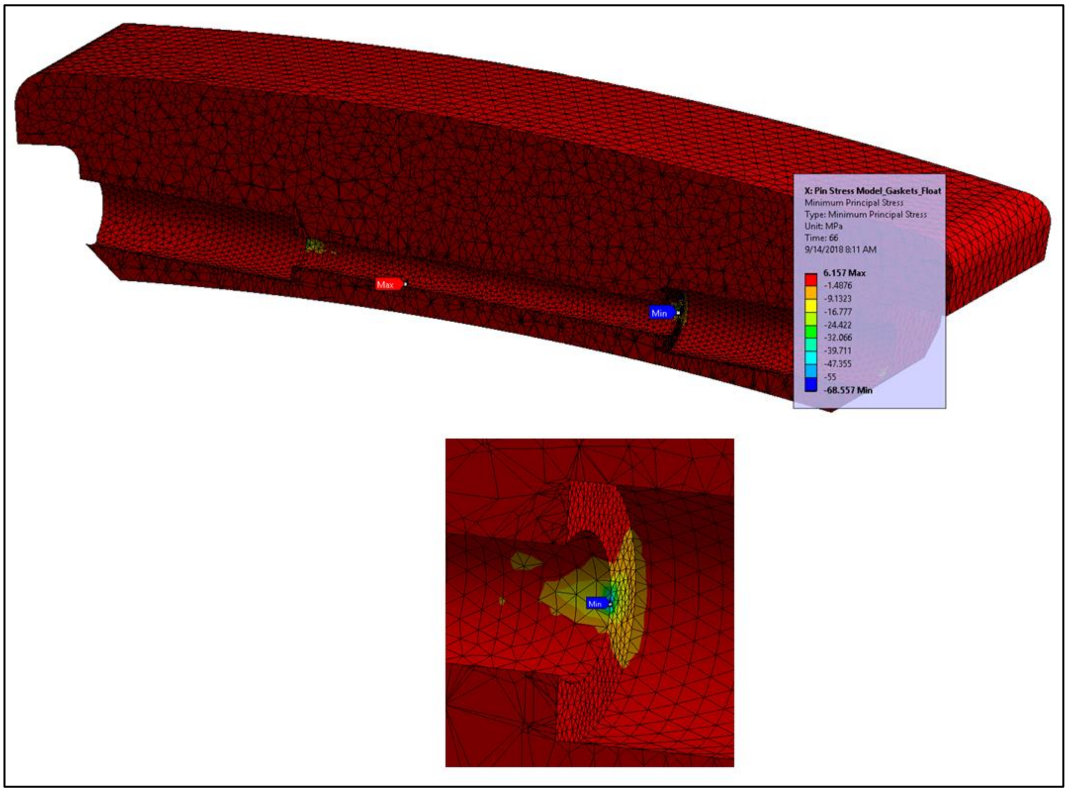

Figure 49: Bolted Tile Redesign, Min. Principal Stress

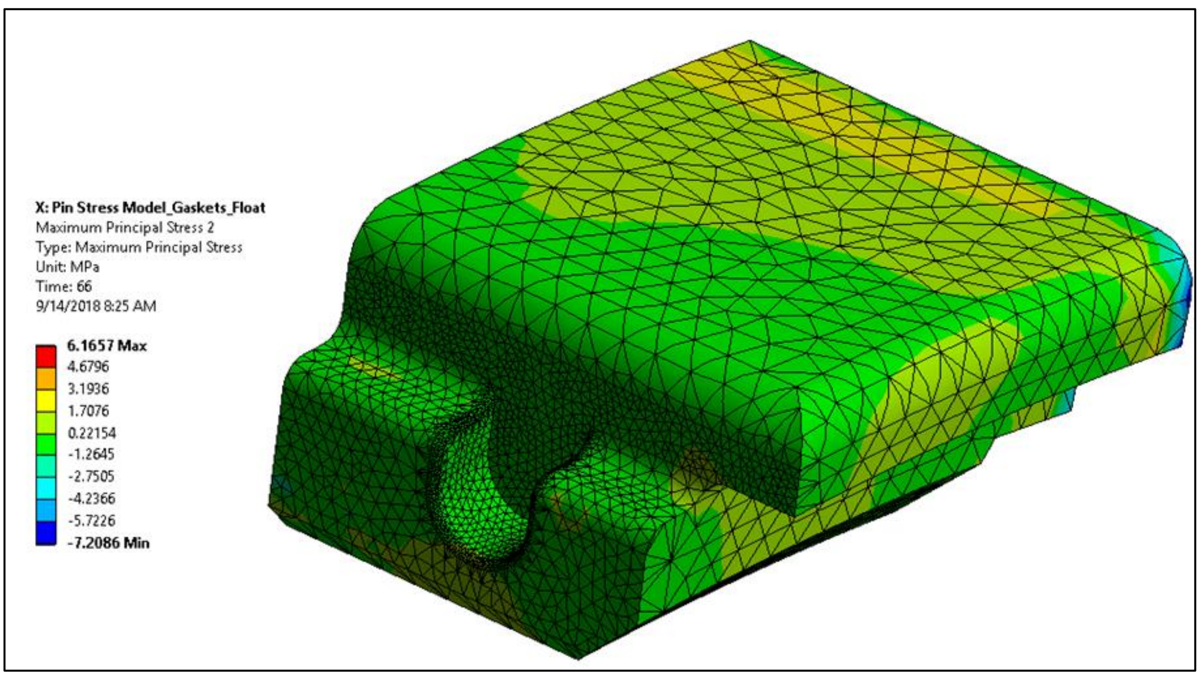

Figure 50: Bolted Tile Redesign, Min. Principal Stress

After the completion of this initial analysis, a global model with the full geometry was also run. A summary of the results from this run are presented in Section 5.

4 Tile Geometric Variants

The tile analysis and results presented thus far were for the “base tile” geometry of the floating tiles. Several other floating tile geometries exist to allow for diagnostic equipment installation.

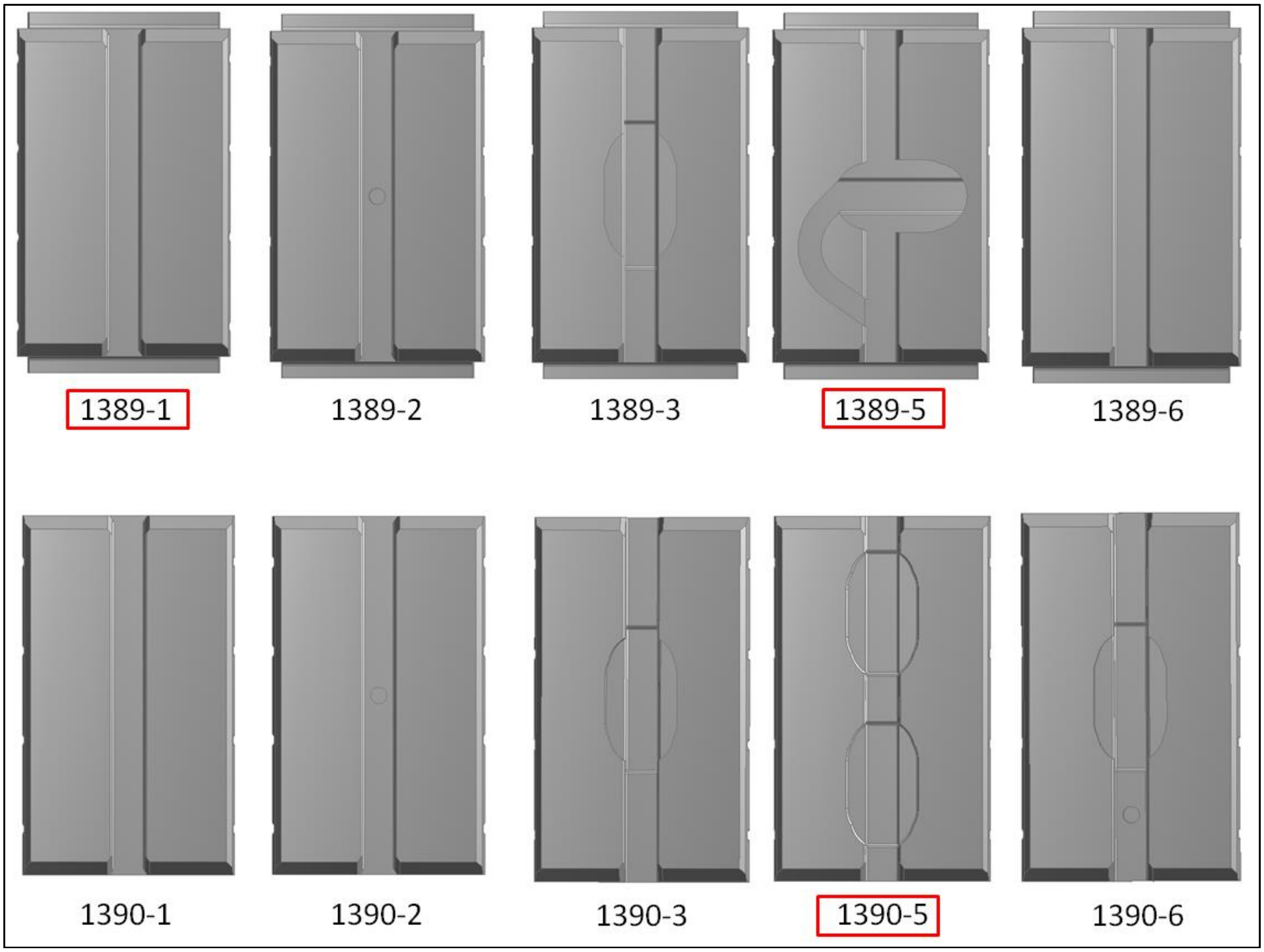

Figure 51: Tile Variations (Figure 1 of 2)

Figure 52: Tile Variations (Figure 2 of 2)

Figure 51 and Figure 52 show the 16 tile geometries. The back sides of the tiles consist of various geometric features for appropriate diagnostic equipment installation. Several of the geometries differ only due to slight dimensional differences between the features.

Ideally, one would perform a combined loading analysis for each one of the 16 tiles. However, the time and resources required for such a task means that this would be an inefficient exercise.

A more reasonable approach would be to perform a full analysis on the base tile, study the results, and then make judicious decisions to select additional tiles for further analysis.

The results for the base tile show that the bulk of the stresses are well below the allowable limits. The only area of high stresses is the pin - pin slot interface. This has been addressed via a design change (Protective gaskets and bushings). However, thermal ratcheting analysis should still be performed on select geometries to rule out issues with temperature ratcheting, regions of temperature spikes and thermal expansion at threaded interfaces. Additionally at least one structural analysis one the tile variants will be performed. The following tile variants were selected for this purpose:

1) **Tile 1389-5**: This is the only floating tile with geometry which is unsymmetrical along the poloidal and toroidal centerlines. Additionally, the curved cut out calls for analysis to determine the thermal response of the geometry.

2) **Tile 1390-5:** This tile has the least mass among all the floating tiles. In addition to thermal ratcheting, a structural analysis was also performed to determine thermal stresses.

3) **Tile 1436-1:** Tiles 1436 and 1437 contain threads for a Langmuir Probe installation. The thermal behavior at the threaded interface and the probe assembly should be investigated.

4.1 Tile 1389-5

The model for the base tile analysis consisted of a full bolted tile and two half floating tiles (one on either side of the bolted tile). This configuration was acceptable due to the geometric symmetry of the floating tiles about the poloidal centerline. For Tile 1389-5, a configuration with a full floating tile and half bolted tiles was used, as shown.

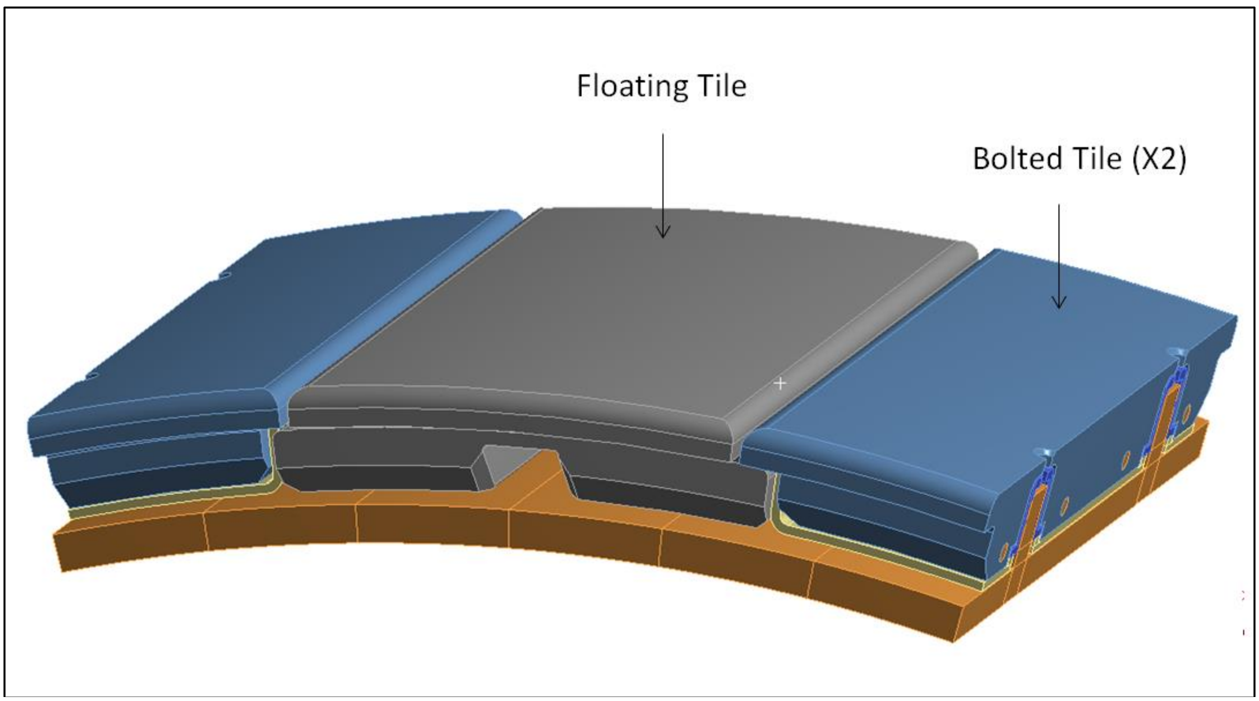

Figure 53: Tile 1389-5 Model Geometry

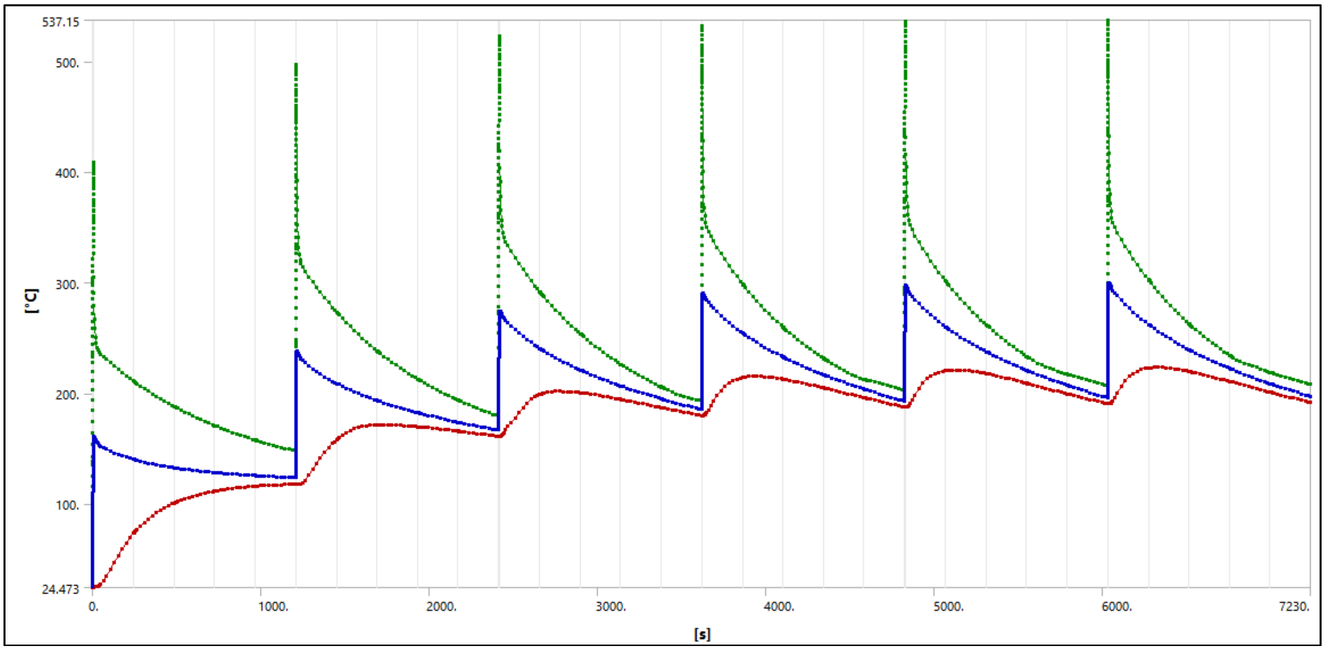

Figure 54: Tile 1389-5 Thermal Ratcheting

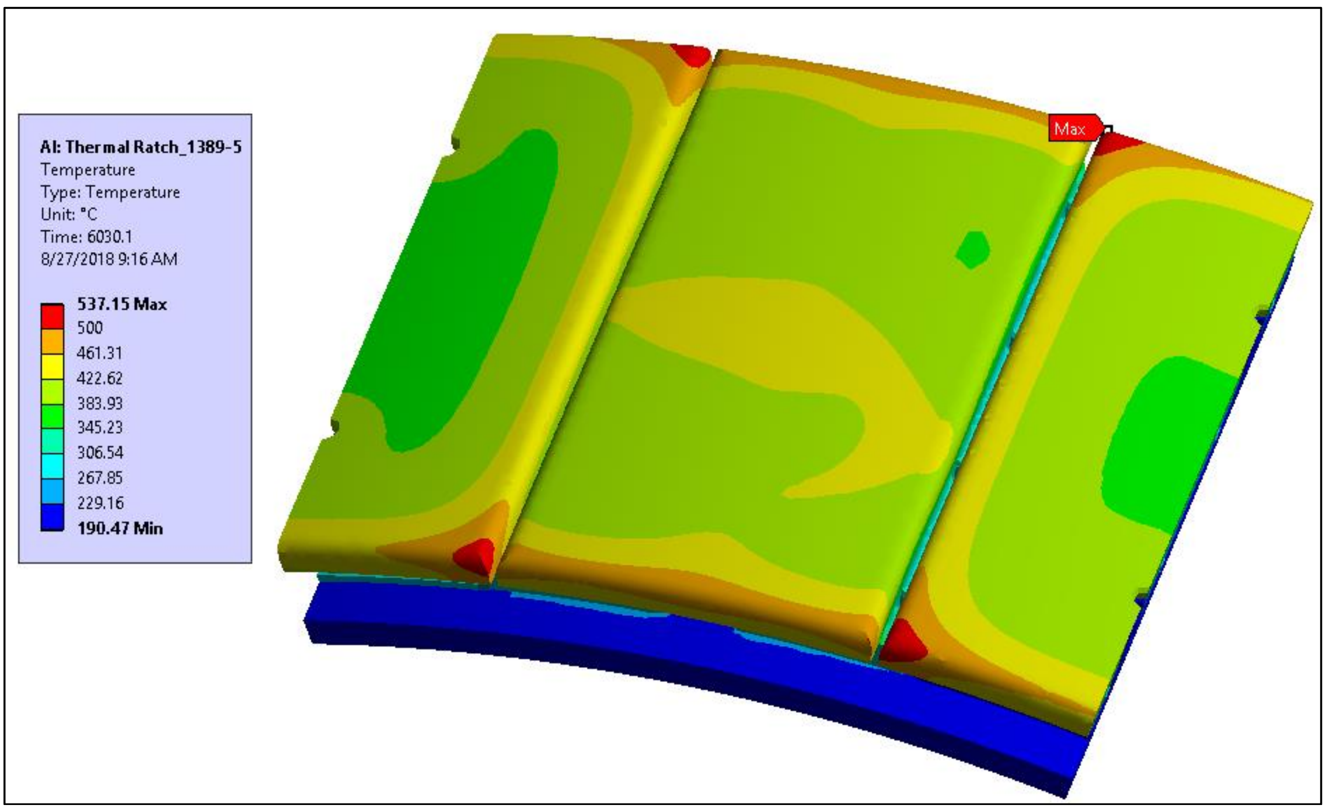

Figure 55: Tile 1389-5 Temperature Distribution at Peak of Last Pulse

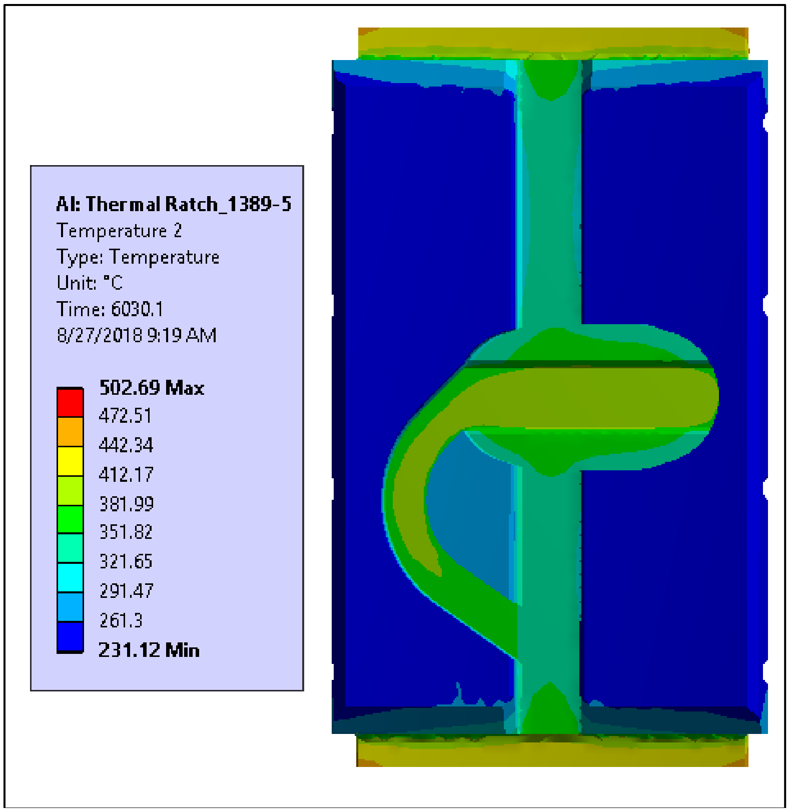

Figure 56: Tile 1389-5 Temperature Distribution – Back Side

The contacts, boundary conditions and input heat flux settings were identical to those for the base tile. The analysis was run for 6 pulses. The system shakes down to a maximum temperature of ~ 537 C (Base tile was ~ 588 C).

4.2 Tile 1390-5

Owing to the symmetric geometry of floating tile 1390-5 it was modeled similar to the base tile – A single central bolted tile and two floating tile halves.

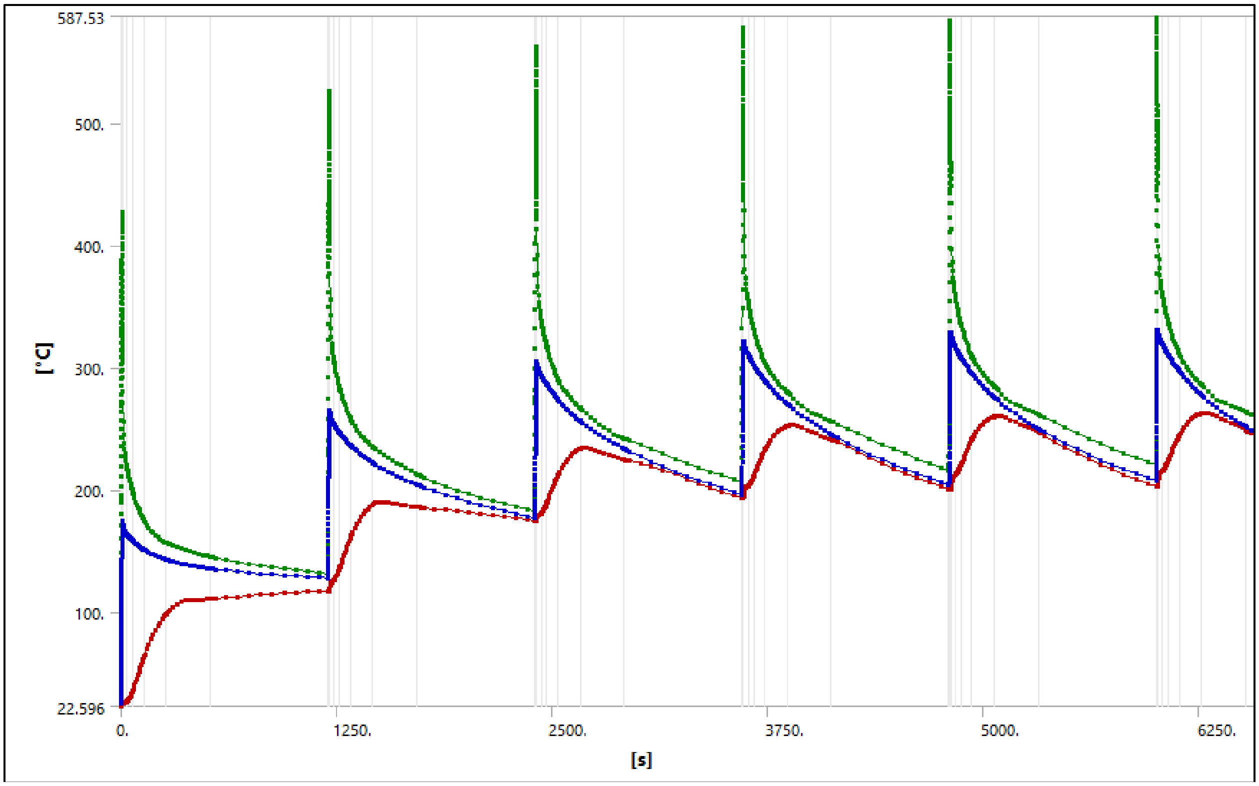

Figure 57: Tile 1390-5 Thermal Ratcheting

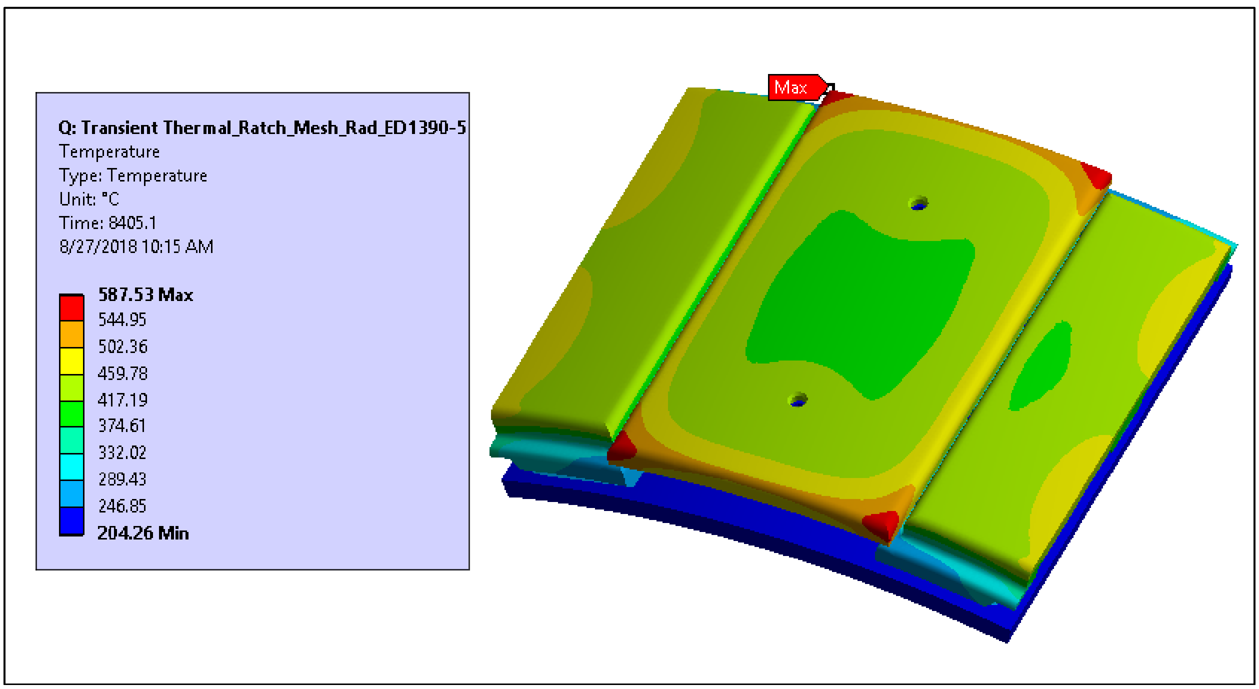

Figure 58: Tile 1390-5 Temperature Distribution at Peak of Final Pulse

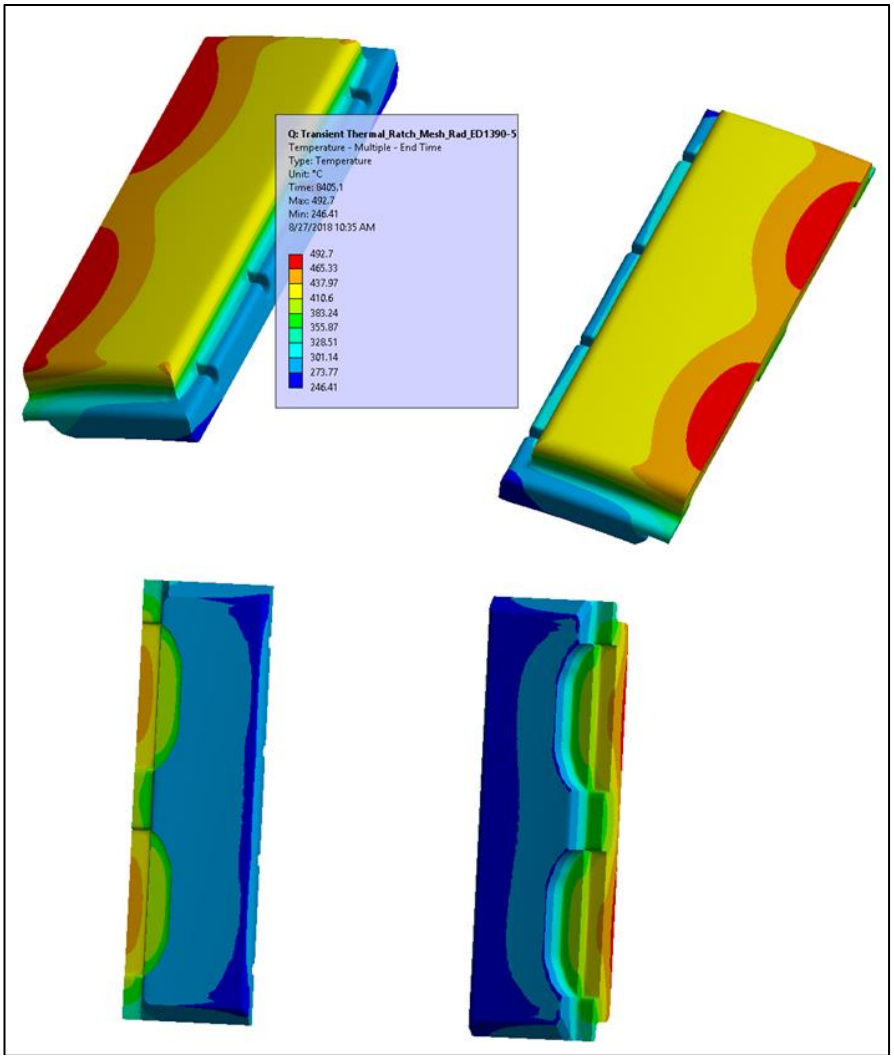

Figure 59: Tile 1390-5 Floating Tile halves Temperature Distribution

The maximum temperature experienced by the assembly is 588 C. The floating tile temperature goes up to ~ 493 C.

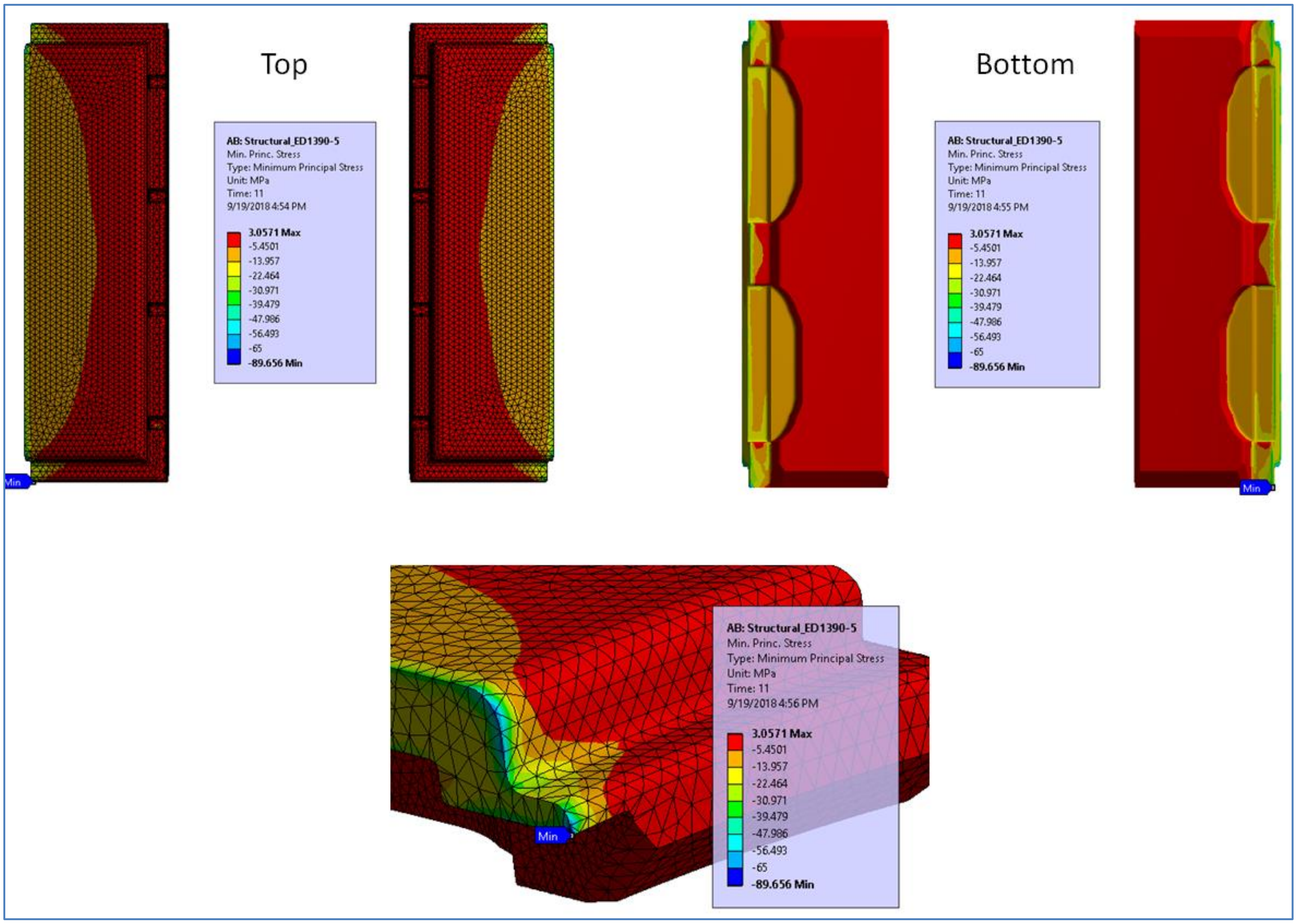

Figure 60: Floating Tile 1390-5 Minimum Principal Stress

The highest compressive stress is seen on a cut surface and is due to the boundary condition on the surface. The bulk compressive stresses are well below the maximum allowable of 65 MPa.

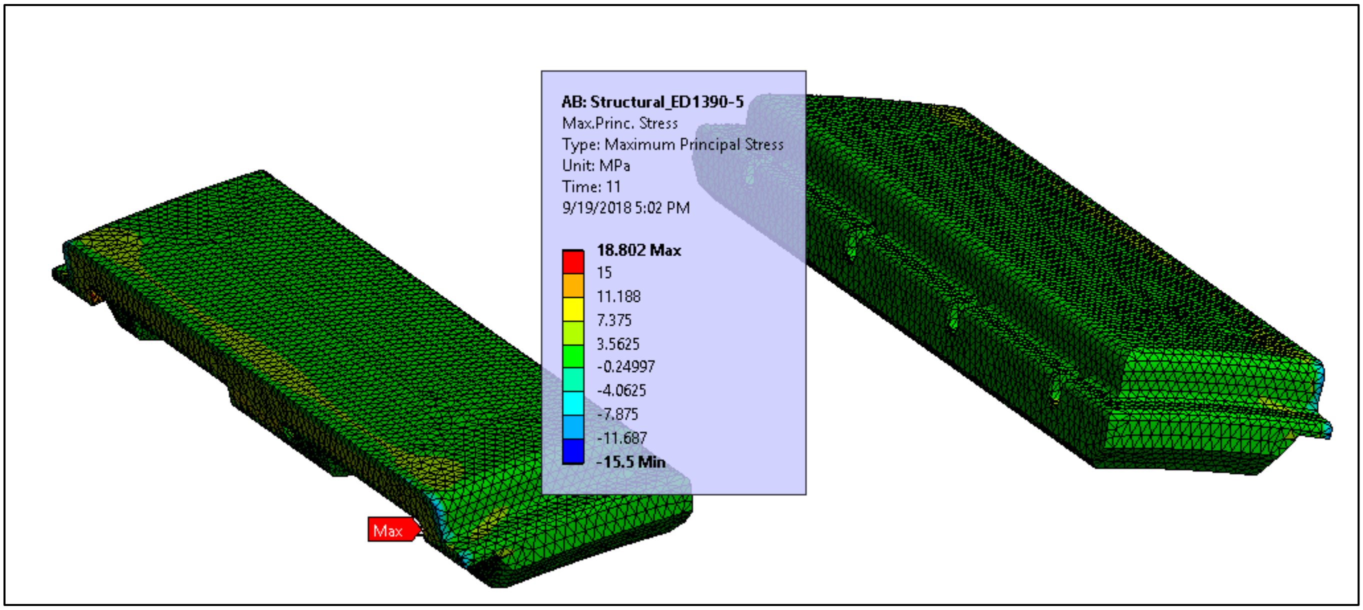

Figure 61: Floating Tile 1390-5 Max. Principal Stress

4.3 Tile 1436-1

Figure 63 shows a cross section of the Langmuir Probe Assembly which will be threaded onto the floating tile. The thread probe plug is the same material as the tile (Graphite 6510). This will ensure uniform thermal expansion at the threaded interface.

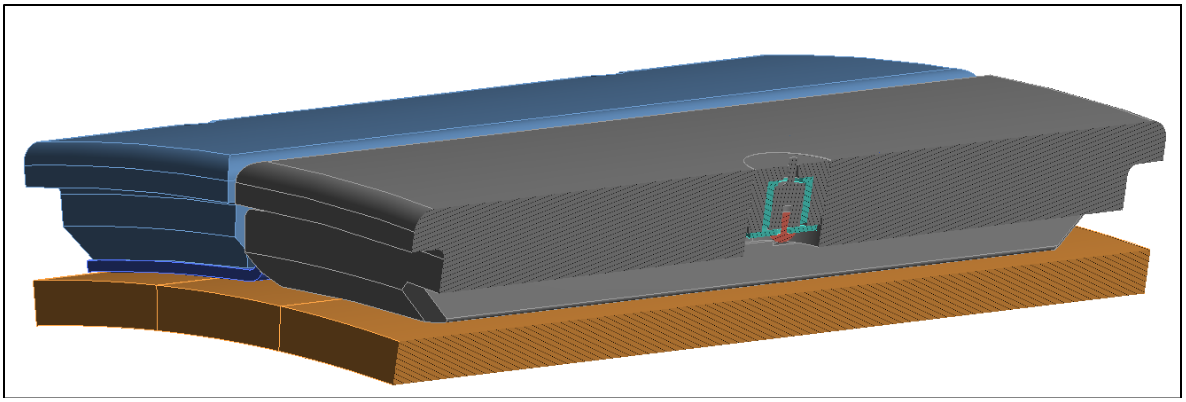

Figure 62: Tile 1436-1 Cross Section

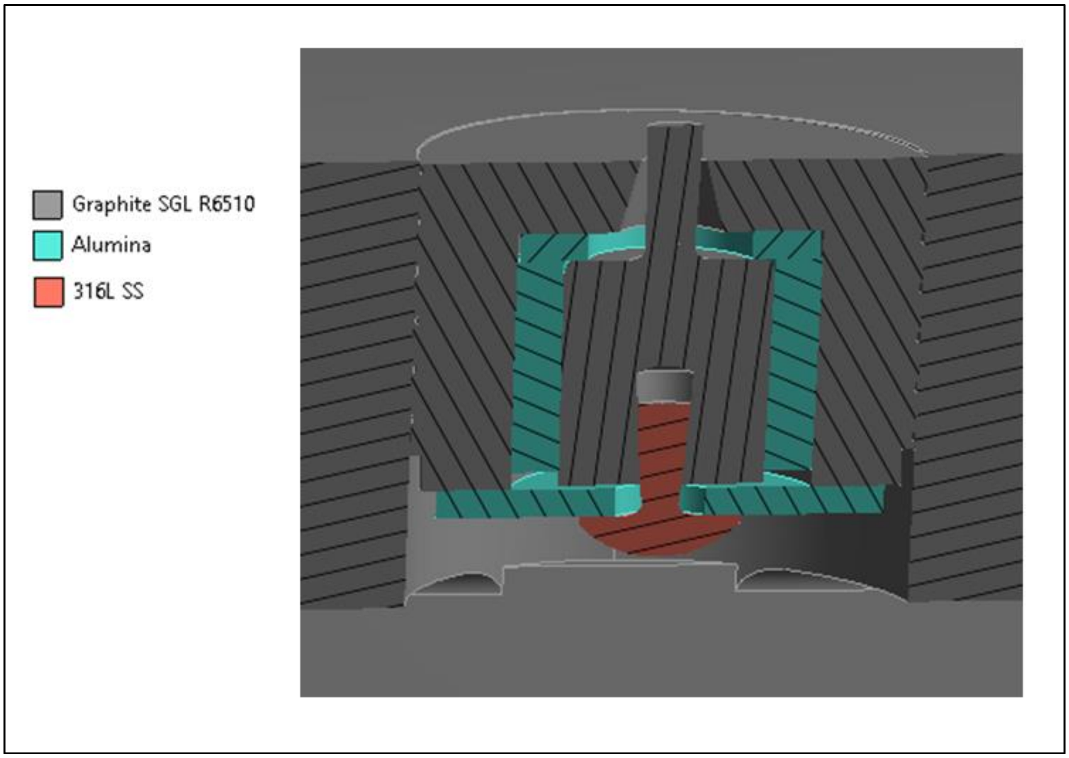

Figure 63: Langmuir Probe Assembly Cross Section

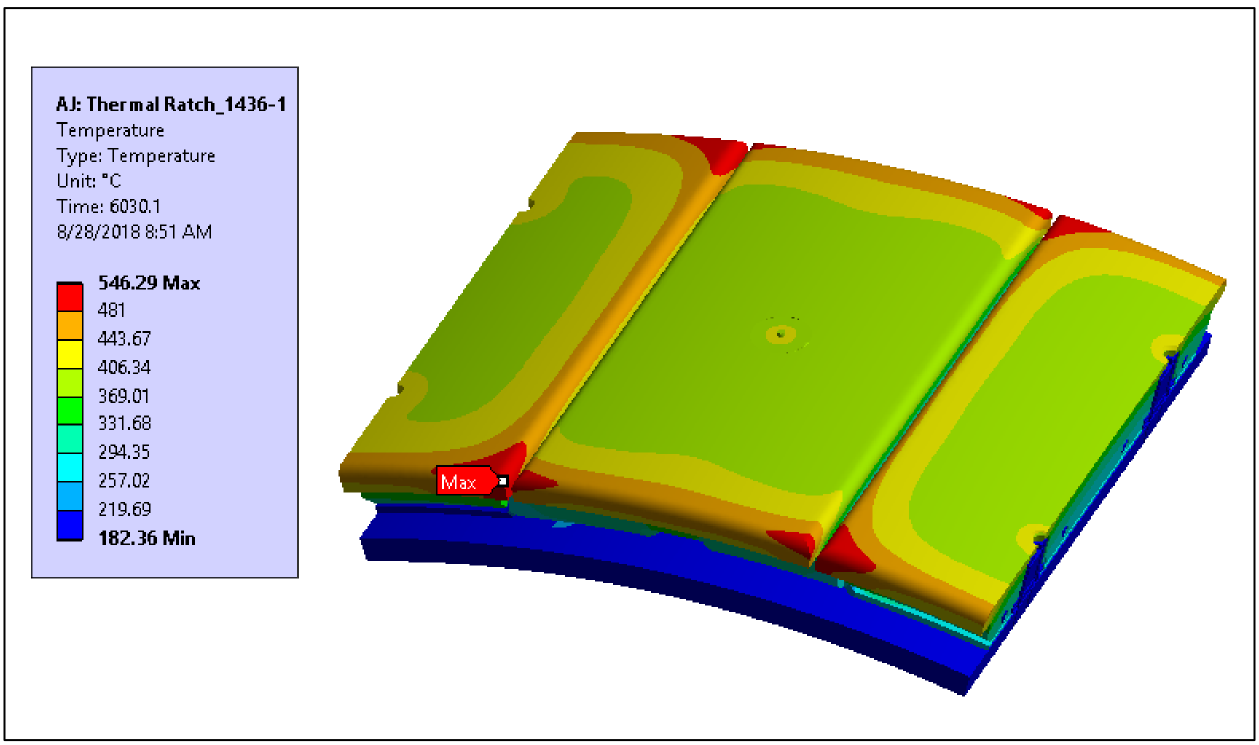

Figure 64: Tile 1436-1 Temperature Distribution at Peak of Final Pulse

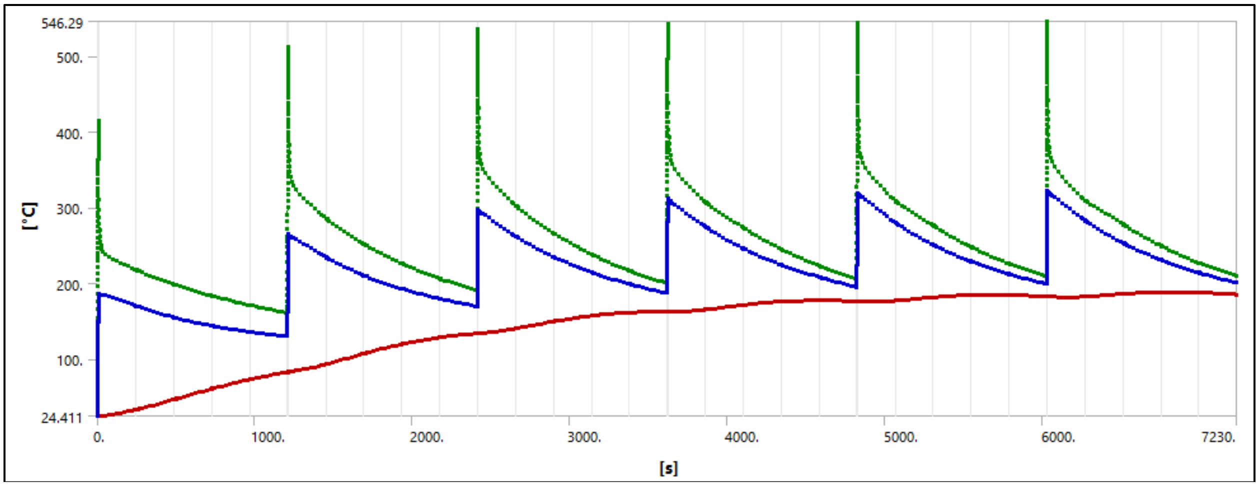

Figure 65: Tile 1436-1 Thermal Ratcheting

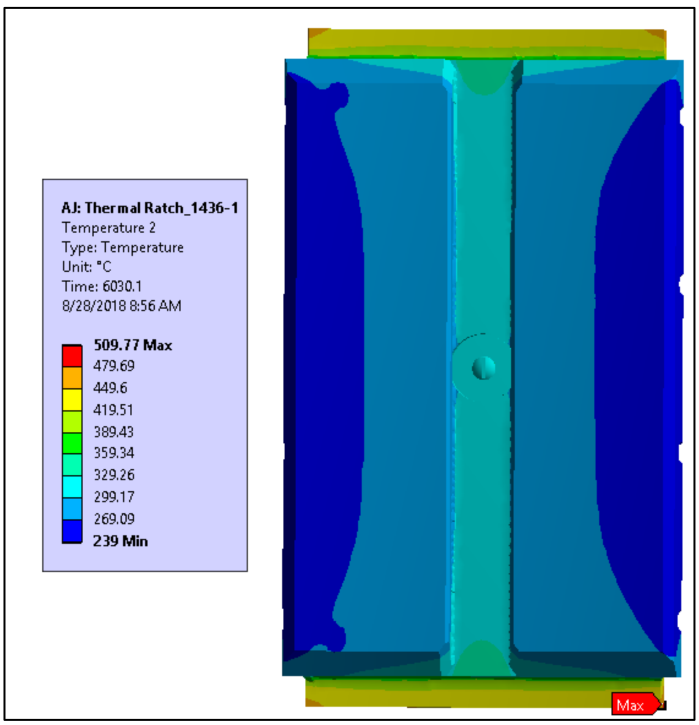

Figure 66: Tile 1436-1 Temperature Distribution – Back Side

5 Full Tile Redesign

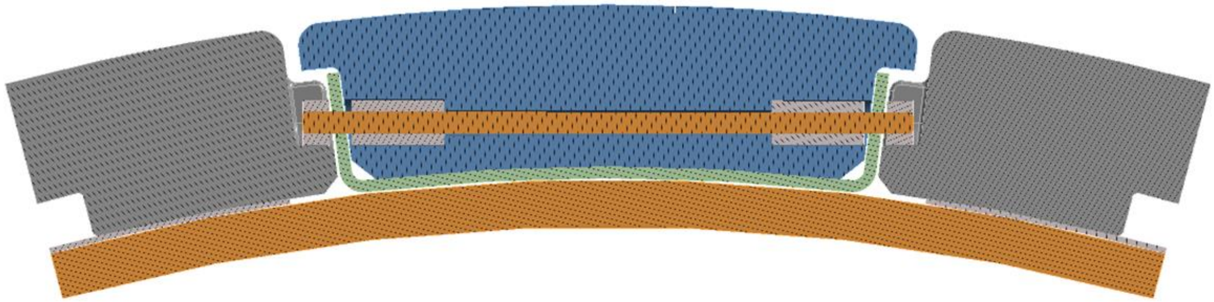

Interface between pin and gaskets was bonded to aid in convergence.

Figure 67: Updated Design Cross Section

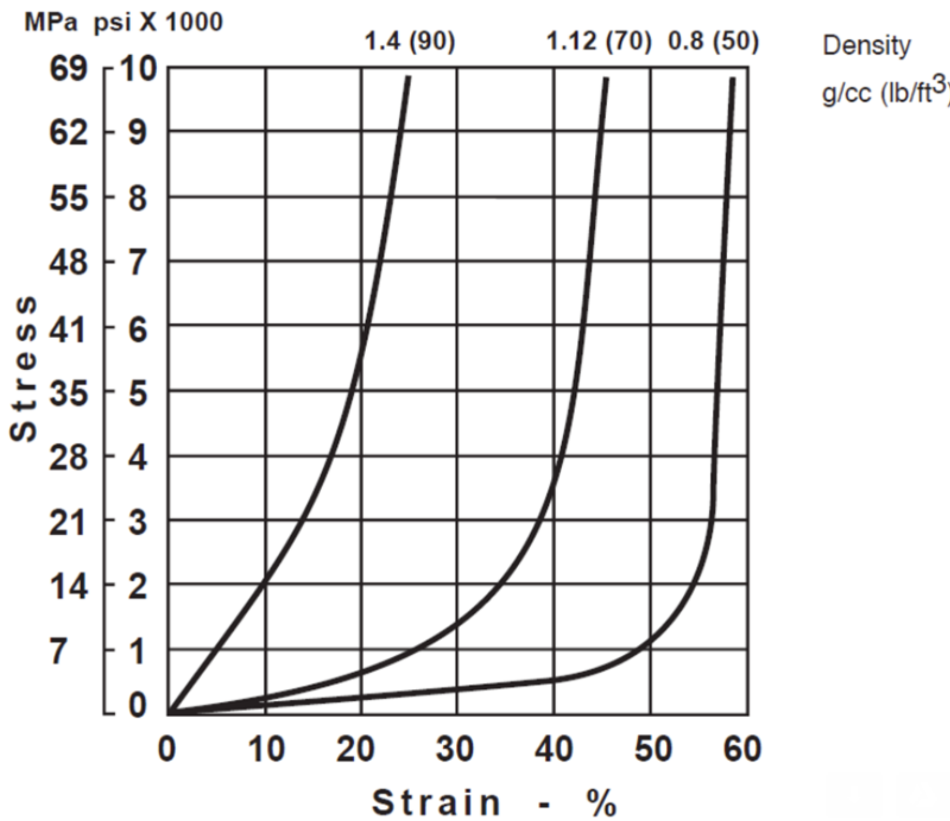

The linear region of the lowest density curve was used (**E = 140 MPa)** for gasket / bushing material.

Figure 68: Gasket Material Curve [Ref?]

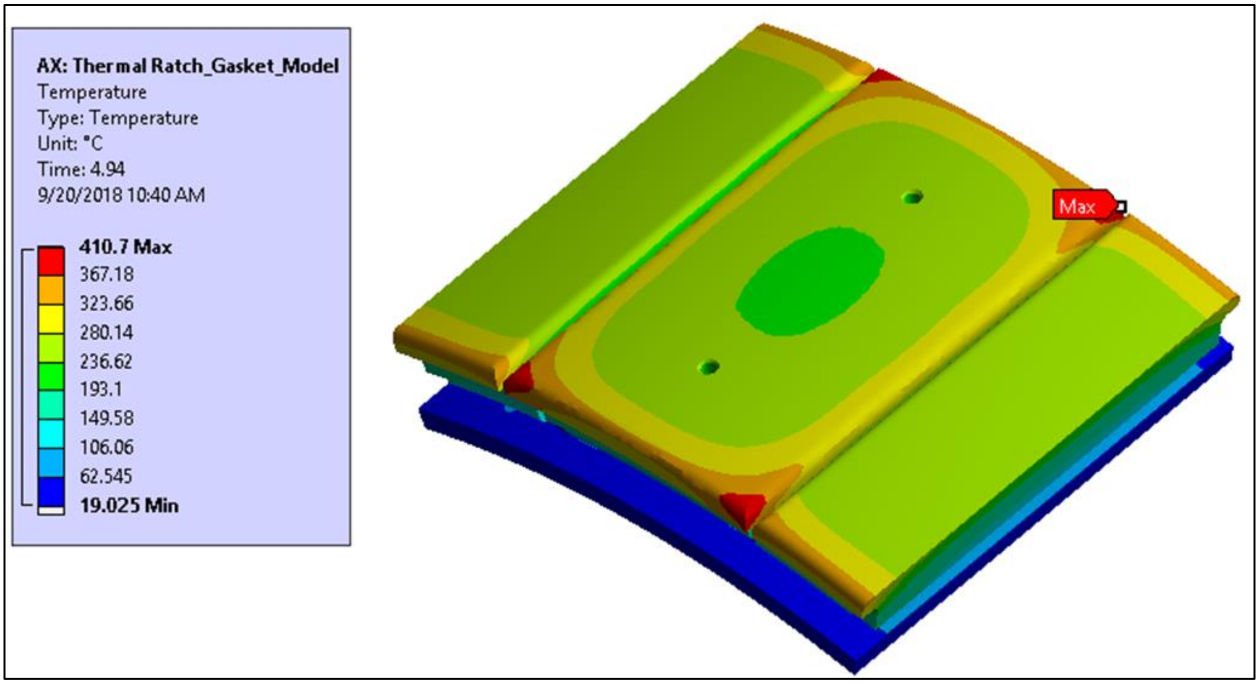

Figure 69: Updated Design Peak Temperature at End of First Halo Pulse

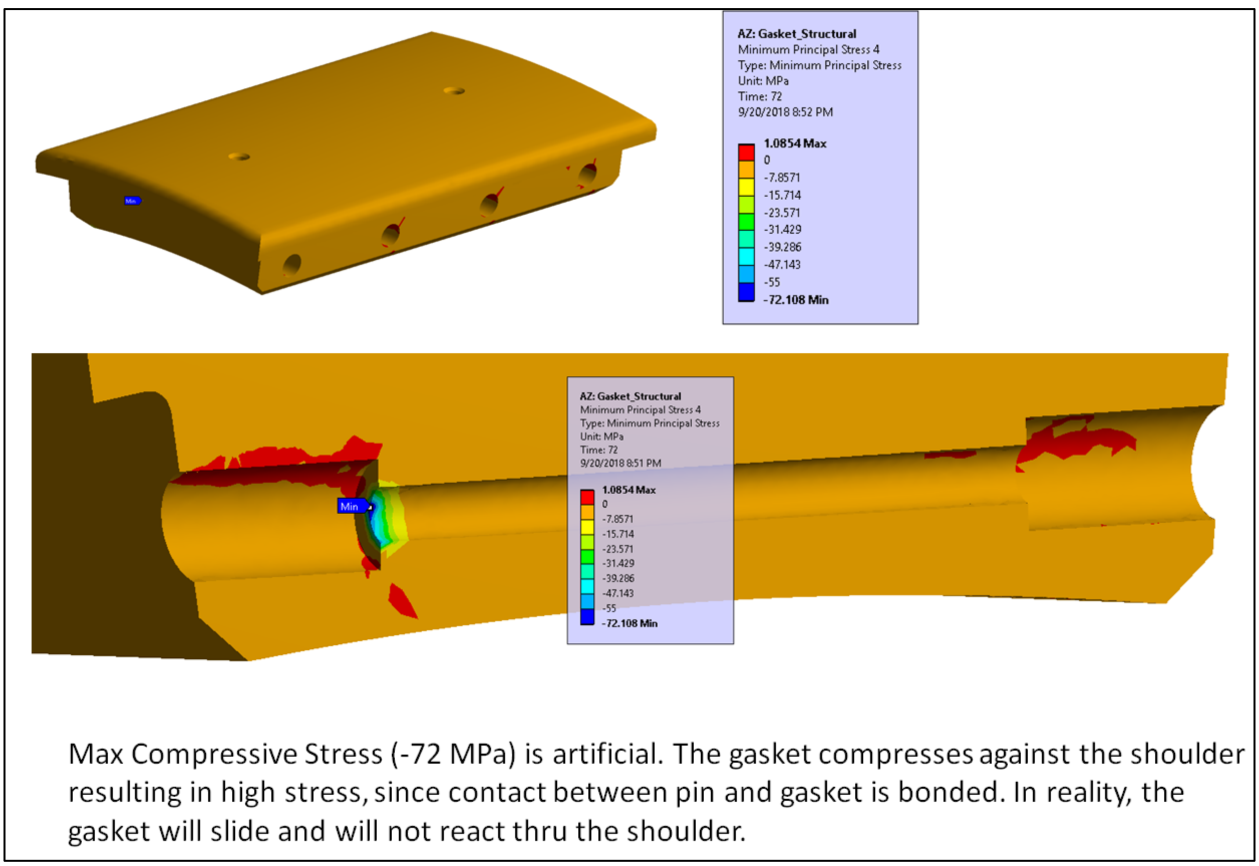

Figure 70: Updated Design, Bolted Tile Min. Principal Stress

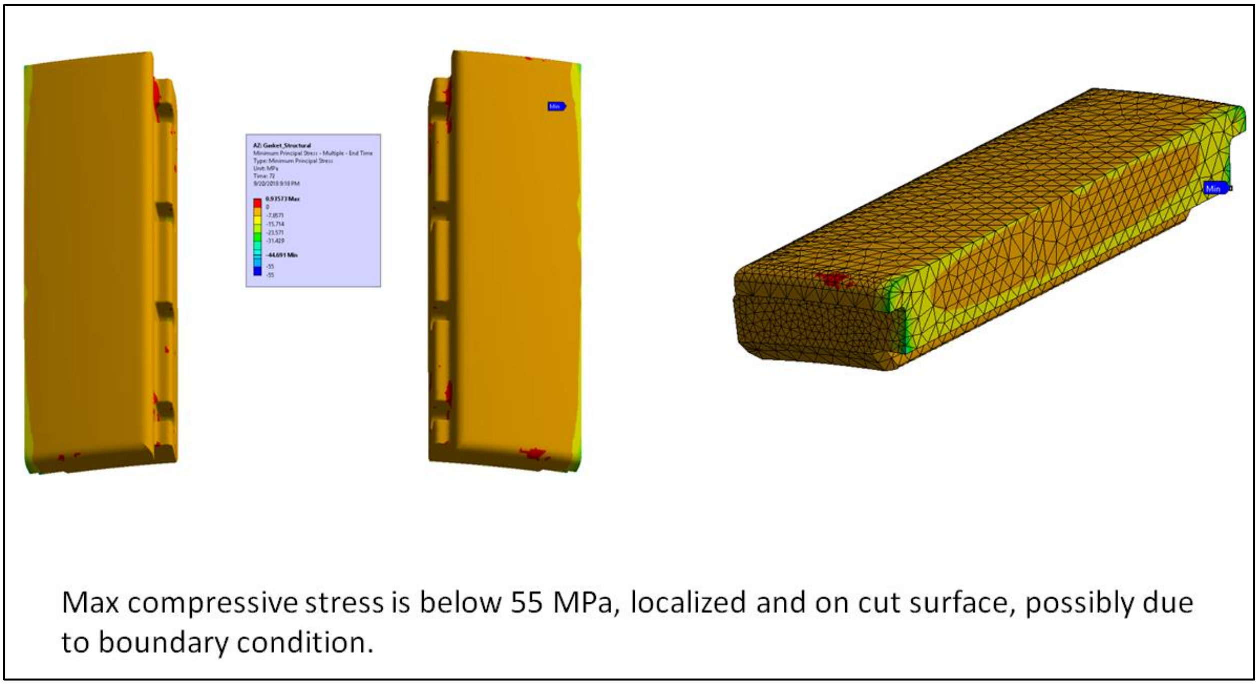

Figure 71: Floating Tile Min. Principal Stress

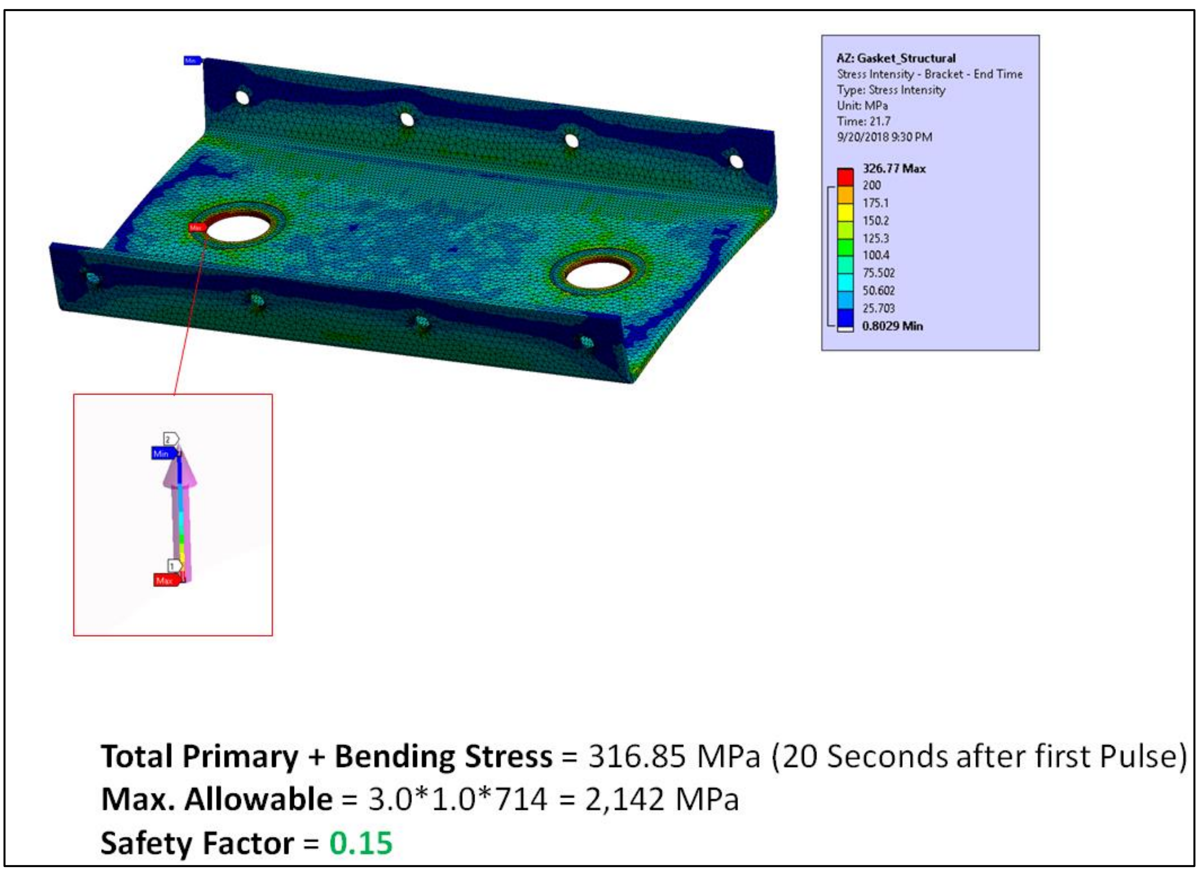

Figure 72: Updated Design, Bracket Maximum Stress Intensity

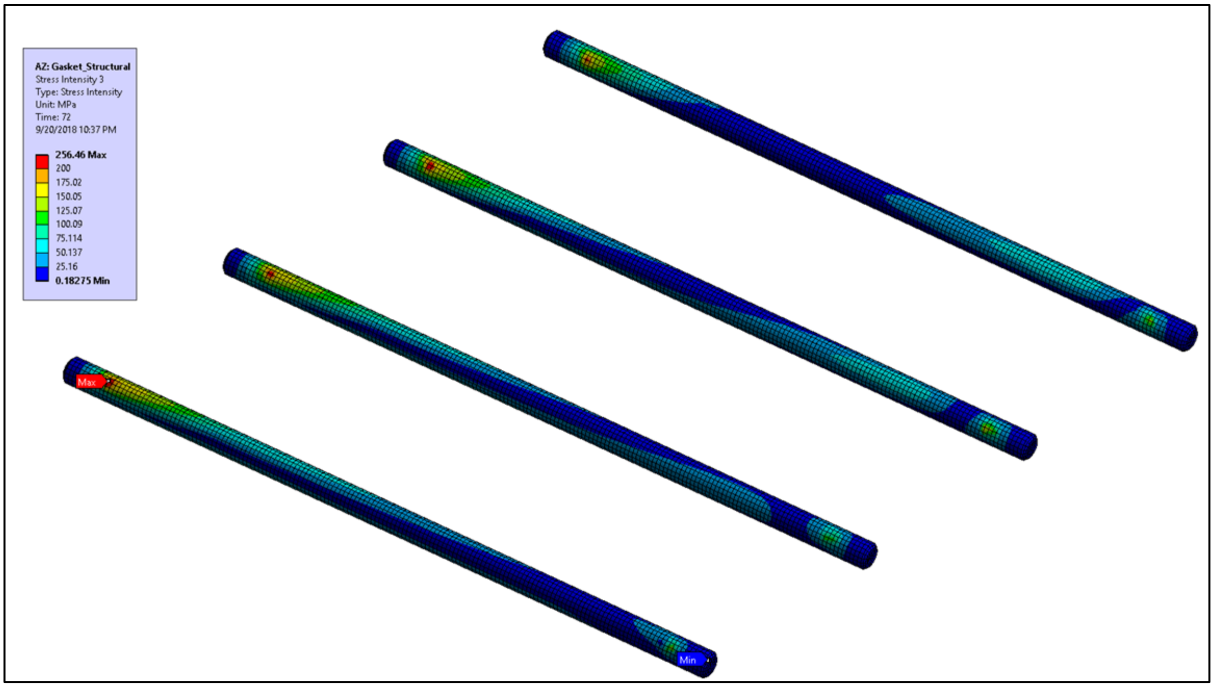

Figure 73: Updated Design, Pins Maximum Stress Intensity

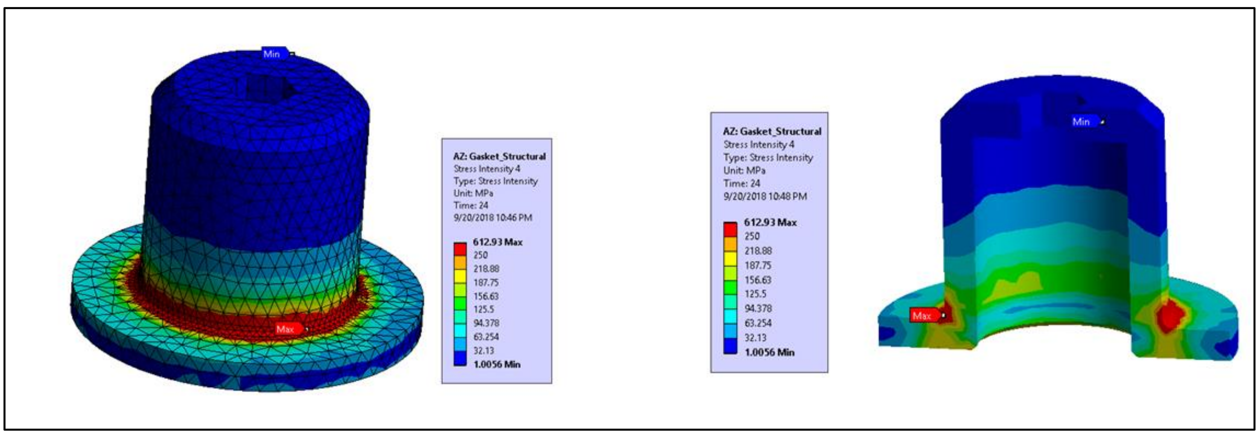

Figure 74: Updated Design, Weld Nut Maximum Stress Intensity

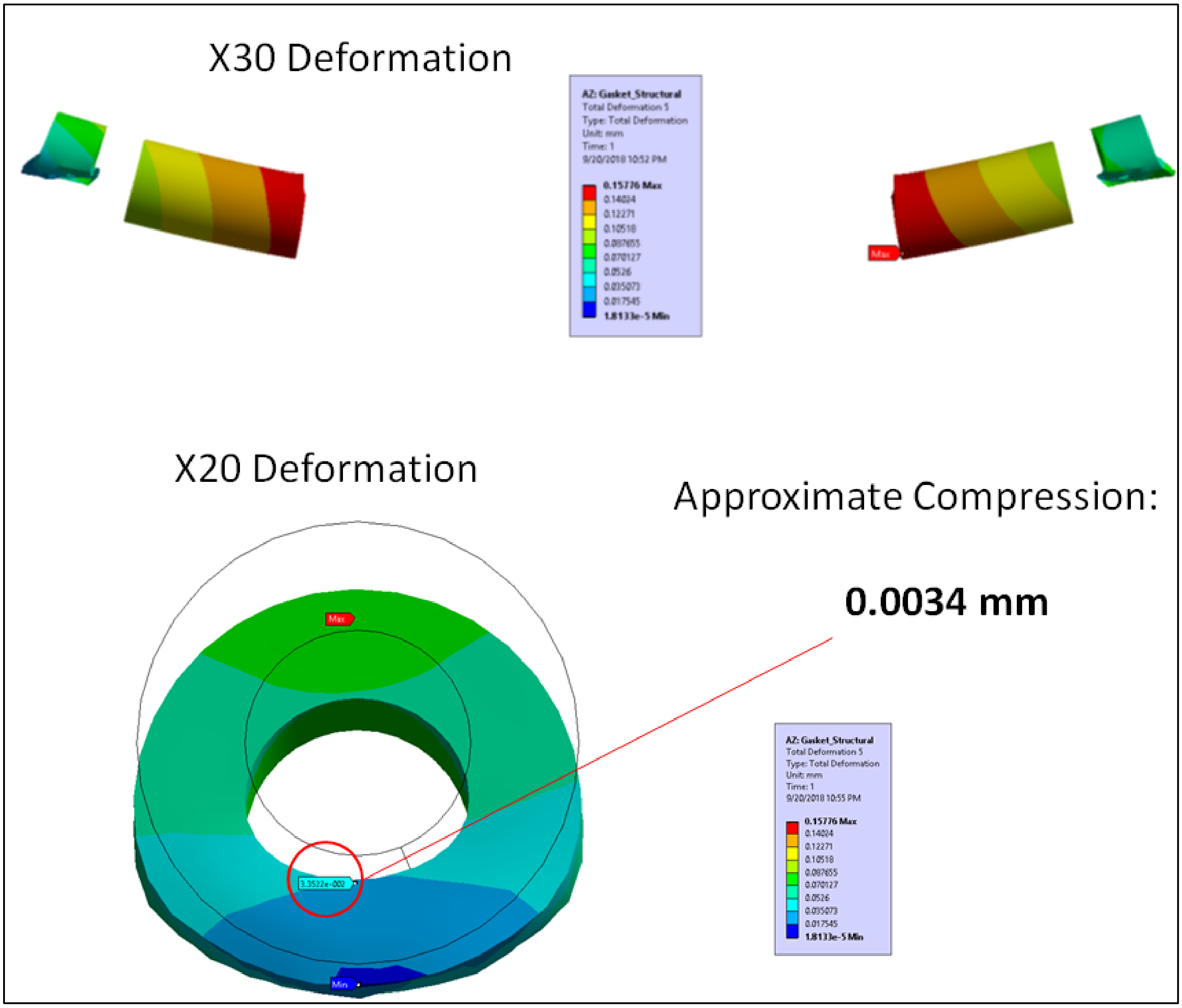

Figure 75: Updated Design, Grafoil Compression at Preload

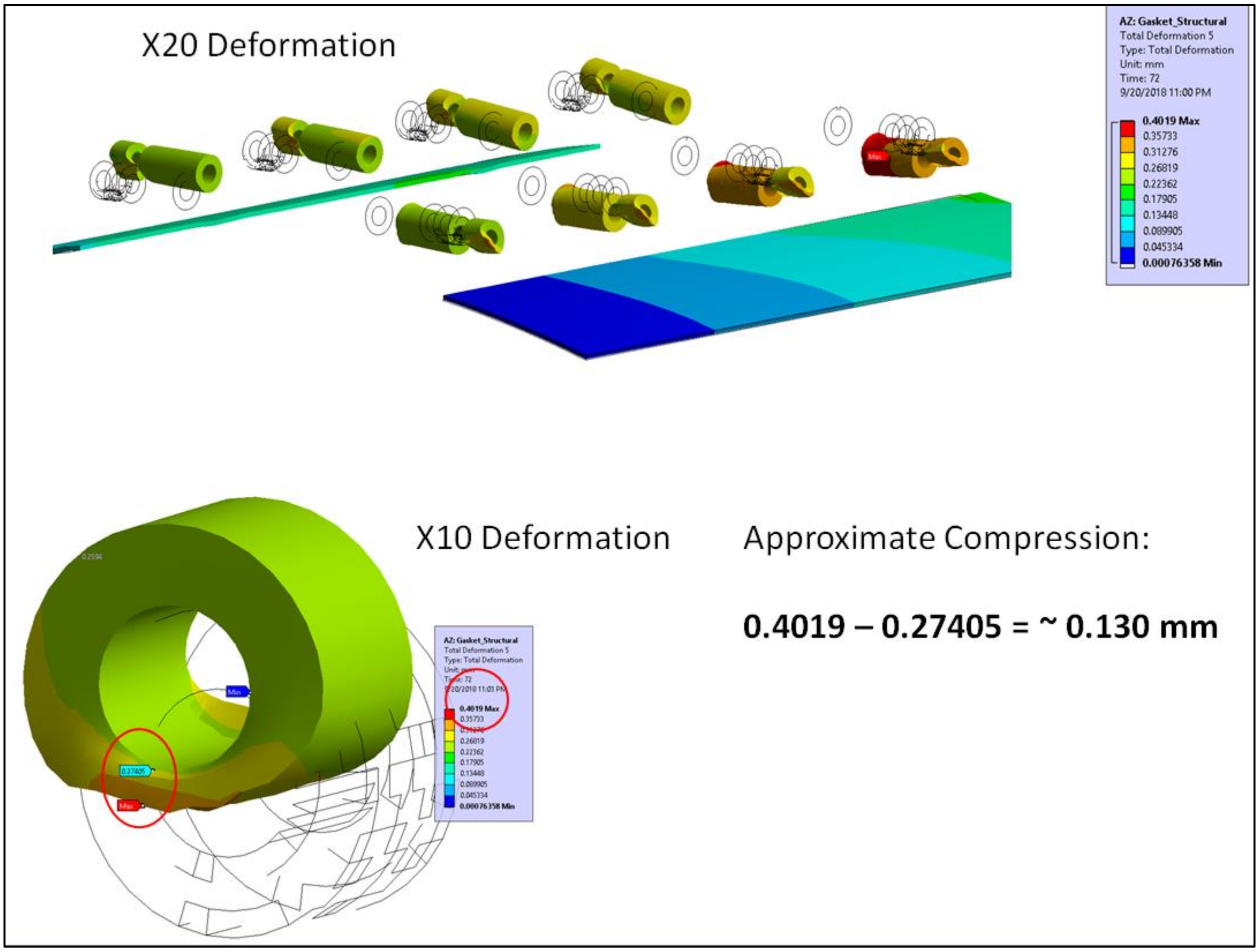

Figure 76: Updated Design, Maximum Grafoil Compression

6 Conclusion

CSFW row 7 – row 21 tiles pass the form, fit and function requirements as laid down by internal PPPL acceptance criteria.

Table 9 shows a summary of the stress results for the metallic components within the PFC assembly. The results are shown as safety factors (Maximum Allowable Stress / Maximum Observed Stress) for Primary Membrane, Primary Membrane + Bending, and Total stress. The allowable stresses are based on the NSTX-U structural design guideline. The pins see negligible primary stress; hence two of the safety factors are listed as N/A.

Table 9: PFC Metallic Components Safety Factors (<1.0 means Pass)

Component	**Pm**	**Pm + b**	**Total**
Bracket	0.17	0.14	0.22
Weld Nut	0.15	0.27	0.87
Washer	0.29	0.34	0.44
Pins	N/A	N/A	0.43

The graphite tiles experience localized compressive stresses which exceed the maximum allowable stress. The tiles cannot be qualified for form, fit and function solely based on the results of this FEA. A design change was made to the bolted tile assembly after this analysis was released. The modified design is acceptable, as documented in the relevant section in this report.